WHOLE BRAIN CHARACTERIZATION OF PERINEURONAL NETS IN THE MALE LONG EVANS RAT

By
Kumarie Budhu

Submitted in partial fulfillment of the requirements for the degree of Master of Art in Biology in the Graduate Division of Queens College of The City University of New York

December 2020

Approved by: _____ (Sponsor) PoKay Ma, Ph.D.

Date: 16th December 2020

Approved by: _____ (Mentor) Joshua Brumberg, Ph.D.

Date: 16th December 2020

Approved by: _____(Committee member) Carolyn Pytte, Ph.D.

Date: 16th December 2020

Table of Contents

Acknowledgements

I would like to thank my mentor, Dr. Joshua Brumberg for guiding me throughout my research career. I would like to thank Dr. Philip Chu for mentoring me and introducing me to the study of PNNs and Dr. Joshua Peck for donating the animals used in this study. I would like to thank Harold Gomes for helping with the statistical model. Thank you, Frank Rotella, for assisting with perfusions and Yakubmier Borukhov for assisting with the counting of PNNs and contouring of cortical regions. Finally, I would like to thank members of the Brumberg lab, and my family and friends for supporting my research work.

This work was supported by PSC-CUNY grant 68793-00-46 and NIGMS 1SC3GM122657 to JCB.

Abstract

Perineuronal nets (PNNs) are specialized extracellular matrix structures of the central nervous system, which predominantly surround inhibitory interneurons. The development of PNNs is activity dependent and relies on sensory input to mature to their adult expression pattern when synaptic circuitry is crystalized following the closure of the developmental critical period. Our results of whole brain characterization demonstrate that the density of PNNs in the neocortex of the Long Evans rat was consistent across animals but varied as a function of the cortical regions analyzed. Given the importance of mystacial vibrissae to the behavior of rodents we further analyzed the laminar distribution of PNNs within the primary somatosensory cortex (S1), known as the barrel cortex. Our results showed that layer 4 of barrel cortex has the highest density of PNNs, followed by layers 5, 2/3, 6 and 1. Within S1, PNN density was consistent across the seven subregions. S1 had a significantly higher density of PNNs than the primary motor (M1) cortex. PNN levels did not show lateralization in either M1 or S1. Interestingly, we also noticed large, brightly stained neurons ensheathed by PNNs that are present only along the layer 6-white matter border. A better understanding of PNNs and their distribution can assist in our understanding of how PNN component manipulation affects neurological conditions such as schizophrenia, epilepsy, stroke and other CNS injury.

Chapter 1: Literature and Background Review

1.1 General Introduction of Perineuronal Nets

The extracellular matrix (ECM) of the central nervous system (CNS) is the non-cellular component surrounding neurons. It is organized in a manner that allows for optimal functioning among all constituents (Pearlman et al., 1996; Wright et al., 2002). The ECM plays key roles in cell proliferation, migration, synaptogenesis, synaptic stability, cell signaling cascades and homeostasis (Dityatev et al., 2003). The components of the ECM are tissue-specific and highly dynamic structures (Frantz et al., 2010). Perineuronal nets (PNNs) are a specific form of the ECM. PNNs were initially discovered by Camillo Golgi in 1893 on neurons of the spinal cord and on the fourth cranial nerve (Celio et al., 1998; Vitellaro-Zuccarello et al., 1998). However, it wasn't until the early 1970's that PNNs reemerged as an area of renewed interest. Initially described as a delicate covering surrounding a neuron, PNNs are now known to form lattice-like structures (Bruckner et al., 1993; Brückner et al., 1998; Celio et al., 1998) around the synapses on the cell body and proximal dendrites of the neurons (Brückner et al., 1998). They have since been studied more extensively in brain development, and plasticity.

Chapter 2: Perineuronal Nets (PNNs)

2.1 PNNs Composition

The components that make up PNNs include chondroitin sulfate proteoglycans (CSPGs) (Bartus et al., 2011; Dityatev et al., 2007), tenascin-R, hyaluronan, and linker proteins (Celio et al., 1998; Carulli et al., 2007) (**figure 1**). Proteoglycans are composed of a core protein and glycosaminoglycan chains that consists of unbranched repeating units of disaccharides. The glycosaminoglycan chains of CSPGs are sulfated with chondroitin sulfate (Wen, et el., 2018; Frantz et al., 2010). CSPGs are members of the lectican family which includes aggrecan, versican, neurocan, and brevican, each exhibiting domain structural similarity. Aggrecan is approximately 220 kDa consisting of an N-terminal hyaluronan (HA)-binding domain and a C-terminal protein-interacting domain (Jones et al., 2010). Hyaluronan is a non-sulfated polysaccharide that surrounds cells and provides compression strength. Versican is about 400 kDa and consists of chondroitin sulfate chains in varying size and length. Neurocan has been implicated in maintaining the PNNs and plays a role in axonal growth (Zhou et al., 2001). The N-terminal side of neurocan in the PNN composition binds to hyaluronan. Hyaluronan is a long polysaccharide synthesized by transmembrane enzymes and it is attached to the cell surface by specific cell receptors. Finally, the initial segments of axons are highly covered by brevican, another chondroitin sulfate proteoglycan (John et al., 2006).

Tenascin-R is a matrix glycoprotein that is exclusive to the nervous system (Anlar and Gunel-Ozcan., 2012) and binds to CSPGs with high affinity (Morawski et al., 2014). Electron microscopy images show that tenascin-R crosslinks the hyaluronan and aggrecan complexes (Lundell et al., 2004) to form the PNN. The linker proteins (Crtl1, Bral1, HAPLN3, Bral2) are present to stabilize the interactions between hyaluronan and the CSPGs by binding to both

(Lundell et al., 2004; Watananbe et al., 1997; Spicer et al., 2003). The link proteins have been implicated in PNN formation in the visual cortex and cuneate nucleus, and animals lacking these proteins have lower levels of PNNs and persistent plasticity (Carulli et al., 2010). These components that make up the PNN are present in many brain regions, although their expression patterns vary diversely throughout the brain (Zimmermann and Zimmermann, 2008; Dauth et al., 2016).

A study in the adult rat cerebellum shows that PNN components are derived from multiple sources; the neurons themselves, surrounding glia, and from afferent synaptic terminals (Carulli et al., 2006). This provides evidence that both neuronal cells and glial cells plays a key role in synthesizing PNN components.

2.2 Enzymatic degradation of the PNN components

Much of our present day understanding of PNNs comes from studies of the enzymatic degradation of the PNN components. The bacterial enzyme Chondroitinase ABC (ChABC), catalyzes the removal of the CSPGs (Yamagata et al., 1968) and is commonly used as a means of degrading PNNs (Brückner et al., 1998; Bradbury et al., 2002; Pizzorusso et al., 2002, 2006). Within the CNS, the term neural plasticity or the critical period of plasticly is used to define nervous system changes following stimulus activity (Mateos-Aparicio and Rodríguez-Moreno, 2019).

Experience-dependent brain plasticity is classically studied in monocular deprivation models. Hubel and Wiesel (1977) examined ocular dominance columns in macaque monkeys following the removal or suturing of one eye post birth. They discovered that the ocular dominance columns of the sutured (deprived) eye decreased in width size while those of the un-

sutured (normal) eye increased in size. In addition, suturing of the eye at two versus three weeks postnatally showed a greater shift in ocular dominance column. This early study was one among many others that provided evidence of neural plasticity and a developmental critical period.

PNN degradation by ChABC in the adult visual cortex (Pizzorusso et al., 2002, 2006) results in reactivated cortical plasticity by restoring ocular dominance plasticity. In the cuneate nucleus of adult rats, PNN degradation leads to sprouting by spinal cord afferent neurons in the denervated brainstem (Massey et al., 2006). Innately, the presence of PNNs significantly reduces neurite outgrowth (Dauth et al., 2016), thus prevent rearrangement in the adult brain and possibly validating why PNNs are deposited later in life as opposed to earlier.

PNNs degradation by ChABC has been shown to affect the neuronal physiology of different classes and subtypes of neurons (Chu et al., 2018). The intrinsic physiology of fast-spiking and low-threshold-spiking interneurons were altered, suggesting that PNNs specifically regulate the intrinsic physiology of inhibitory interneurons.

The components of PNNs are involved in the pathological processes of CNS disorders (see below). The manipulation of CSPGs is believed to have therapeutic potential for certain CNS disorders such as epilepsy, stroke and Alzheimer's disease (Galtrey et al., 2007). At injury sites in cases of CNS injury, CSPGs are highly expressed and implicated in the inhibition of sprouting (Massey et al., 2016). PNN degradation by modification of CSPGs have demonstrated reparative effects associated with functional recovery (Romberg et al., 2013; Massey et al., 2006; Galtrey et al., 2007; Bartus et al., 2011). Thus, understanding the distribution of PNNs in the brain may provide insights into brain functioning and pathology.

2.3 Methods of PNN Visualization

Wisteria floribunda agglutinin

Wisteria floribunda agglutinin (WFA) is a plant lectin most commonly used to visualize PNNs. WFA preferentially binds to the N-acetylgalactosamines beta 1 (GalNAc beta 1–3 Gal) residues of glycoproteins in the ECM surrounding neurons (Hartig et al., 1992; Brückner et al., 1993; Hilbig et al., 2001). WFA labeling produces an intensity profile along the cell showing the lattice like assembly of the PNNs, defined by CSPG binding (Tewari and Sontheimer, 2019). The staining intensity of WFA is still a contested matter but one prominent hypothesis states that more brightly stained PNNs by WFA fluorescence intensity corresponds to mature PNNs while decreased WFA intensity corresponds to more immature PNNs (Wang and Fawcett, 2012; Slaker et al., 2016).

PNNs can also be visualized using monoclonal and polyclonal antibodies to chondroitin sulfate proteoglycans (Lander et al., 1997), such as the monoclonal antibodies Cat-301, Cat-315, and Cat-316 (Matthews et al., 2002). WFA-negative PNNs for instance, are found on certain neuron subtypes and do not bind to WFA, but instead only to the aggrecan antibodies (Matthews et al., 2002).

2.4 PNNs Development

Normal brain development begins prenatally and extends to postnatal life with developmental similarities between rodents and humans (**figure 2**). The developmental critical period is a time sensitive postnatal temporal window during which environmental stimulus has the strongest influence on neurons thereby altering synaptic networks in response to environmental input. Synaptic pruning is a developmental strategy common to humans, primates

and rodents (Anderson, 2003) resulting in refinement of the synaptic circuitry (Semple et al., 2013). This activity-dependent process is associated with brain plasticity, and in rodents PNN maturation is concurrent with the closure of this developmental critical period. Many studies (Anderson, 2003) have demonstrated that synaptic morphology varies across brain regions within the human cortex at different time points, which might provide an alternative hypothesis for varying levels of PNN expression in different cortical regions.

In rodents, PNNs appear after the first three to five weeks of postnatal development and reach their mature expression when the synaptic circuitry is established (Carulli et al., 2006; Ye and Miao, 2013). Between postnatal day (PD) 14 to 28, Lipachev et al. (2019) reported a gradual increase of PNNs in the mouse somatosensory cortex. However, PNN density may still continue to increase within the visual and somatosensory cortices of older mice (Kaertko-Sysa et al., 2014).

Bruckner et al. (2000) showed that the earliest differentiating PNNs appeared in the brainstem regions, including the red nucleus, medial nucleus of the trapezoid body, and the gigantocellular reticular nucleus, at postnatal day 7, but PNNs in the barrel field of the somatosensory cortex first appears on postnatal day 14. In the rat spinal cord, PNNs first appear on PD 7 and reach their mature expression by PD 21 (Galtey et al., 2009).

PNNs have also been reported even earlier at PD 10 in the mouse somatosensory cortex in other studies (Nakamura et al., 2009). In the mouse visual cortex, a small density of PNNs were visualized starting at PD 10 and their density increased from PD14 until reaching a plateau around PD42; thus, correlating PNN maturation and the developmental critical period within the visual cortex (Ye and Miao, 2012).

2.5 PNN Localization

Within the CNS, PNNs exhibit cell-type specificity (Lensjo et al., 2017) and are preferentially associated with GABAergic interneurons (Hensch, 2005). PNNs primarily surround the cell bodies of fast-spiking (Balmer et al., 2009) parvalbumin (PV+) expressing inhibitory interneurons (Alpár et al., 2006, Brückner et al., 1993; Bertolotto et al., 1996; Celio et al., 1998; Celio et al., 1993, McRae et al., 2007; Celio and Chiquet-Ehrismann, 1993; Hartig et al., 1992; Kosaka and Heizmann, 1989). Parvalbumin (PV) is a calcium binding protein. Both PV-positive interneurons and PNNs have been shown to exhibit parallel maturation around the closure of the developmental critical period (Pizzorusso et al., 2002; Ye and Miao, 2013). As such, PV+ cells have been suggested as regulators of brain plasticity (Hensch, 2003).

However, this colocalization is not evident in all brain regions and the strength of the correlation varies in rats versus mice (Lensjo et al., 2017). In one study, Lensjo et al. (2017) investigated the expression patterns of PNNs in the visual cortex, hippocampus and the medial entorhinal cortex (mEC). Unlike the other cortical regions, the hippocampus has a very low PNN density with PNNs present in all subregions of the hippocampus in mice but only in the CA2 and CA3 subregions of the hippocampus in rats. In the visual cortex PNNs almost exclusively colocalized with PV+ interneurons in both rats and mice but in mEC it was found that PV+ interneurons colocalized with PNNs more with mice than with rats.

Although PNNs have the highest level of co-localization with Parvalbumin expressing interneurons, they can also be found around other cell types. In the mEC for example, PNNs are shown to overlap with reelin-positive cells and calbindin expressing cells. PNNs also colocalize with CaMKII and PCP4-expressing neurons in CA2 of the hippocampus (Lensjo et al., 2017).

2.6 PNN Functionality

In recent years, there has been increased focus on PNN functionality because of their role in synaptic plasticity (Karetko and Skangiel-Kramska, 2009) and degradation in neural pathologies (Galtrey et al. 2007; Massey et al., 2016). The exact function of the PNN is unclear however, they are involved in synaptic stabilization (Kwok et al., 2010; Hensch, 2003; Fawcett, 2009), neurotransmitter receptor mobility and the inhibition of plasticity (Bukalo et al., 2001; Frischknecht et al., 2009; Pizzorusso et al., 2002, 2006; Carulli et al., 2016).

PNNs are composed of proteoglycans and polysaccharides which give the cell surface a strong negative charge (Seeger et al., 1994; Morawski et al., 2004, 2015). Based on their negatively charged structure, PNNs have been hypothesized to act as a buffering system for cations (Bruckner et al., 1993) and as a protection for neurons against oxidative stress (Morawski et al., 2004). Chu et al., 2018 demonstrated that the ChABC digestion of PNNs resulted in neuron specific impacts of intrinsic and synaptic properties, specifically of fast spiking and low threshold spiking interneurons. However, while PNNs maintain the extracellular space, they also serve as diffusion barriers through electrostatic interactions (Morawski et al., 2015). It is likely that through those interactions, PNNs are able to accumulate local molecular gradients of cationic molecules such as calcium. Thus, PNNs can act through parvalbumin positive interneurons to potentially limit plasticity (Lensjo et al., 2017; Morawski et al., 2015). PNNs are also thought to directly restrict plasticity by physically obstructing novel synaptic connections and preventing axonal sprouting.

2.7 PNNs and Pathology

PNNs have been implicated in a variety of neurodegenerative and neurodevelopmental disorders. Many studies have indicated that it is the ECM molecules that are involved with PNNs

that may be the implicative factor in many psychiatric disorders, such as schizophrenia, Alzheimer's disease, and mood disorders (Pantazopoulos and Berretta, 2016). Below I will provide a short description of the role the PNNs plays in the pathophysiology of various psychiatric disorders and neurological processes.

Autism Spectrum Disorders

Autism spectrum disorders are a group of neurodevelopmental disorders spanning a continuum and largely affecting communication and behavior. Of the interconnected ECM, additional molecules including the hyaluronan surface receptors CD44 and OTX2, RELN, SEM3A, SEM4D, and the ECM remodeling enzymes ADAMTS3, ADAMTS5, ADAMTS14 have been implicated in autism genome-wide association studies (summarized in Pantazopoulos and Berretta, 2016).

A reduction in reelin, a glycoprotein previously found to overlap with PNNs (Lensjo et al., 2017), has also been implicated in autism (Fatemi et al., 2001; Pantazopoulos and Berretta, 2016). Heparan sulfate proteoglycans, like chondroitin sulfate proteoglycans are both highly negatively charged glycosaminoglycans with acidic sugar residues and sulfate groups (Park et al., 2017) that comprise the PNN. This complex polysaccharide is also decreased in autism (Pantazopoulos and Berretta, 2016).

Fragile X Syndrome

Fragile X syndrome is a genetic disorder resulting in intellectual disability. The matrix metalloproteinase, metalloproteinase-9 (MMP-9) is a zinc-dependent endopeptidase that degrades ECM proteins and regulates tissue remodeling (Yabluchanskiy et al., 2013). Fragile X

syndrome occurs as a result of transcriptional silencing of the *Fmr1* gene, which produces the Fragile-X mental retardation protein, a mRNA binding protein (O'Donnell and Warren ST, 2002). MMP-9 is implicated in Fragile X syndrome (Pantazopoulos and Berretta, 2016) through the Fragile-X mental retardation protein and MMP-9 interactions, by upregulation of MMP-9 and subsequent Fragile X abnormalities. FMR1 knockout mice reveals reduced PNN formation around GABAergic interneurons in the auditory cortex (Wen et al., 2018). Subsequent genetic reduction of MMP-9 to wild type levels resulted in restoration of PNN levels in the auditory cortex. Thus, PNNs are expressed in an MMP-9 dependent manner and increase of MMP-9 level results in sensory hypersensitivity.

Mood Disorders

Mood disorders, such as bipolar disorder and major depression are another category of psychiatric disorders that are associated with PNNs. In the amygdala of postmortem subjects with bipolar disorder, Pantazopoulos et al. (2015) reported a decrease in PNNs levels. Reelin expression has also been shown to decline in in the prefrontal cortex, hippocampus, and cerebellum of postmortem subjects with bipolar disorder and depression (Fatemi et al., 2000). Specific markers of chondroitin sulfate PNNs are lower in bipolar disorder in the amygdala (Pantazopoulos et al., 2015). In addition, an upregulation of MMP-9 in subjects with major depression and bipolar disorders have been reported (Rybakowski et al., 2013), further providing evidence for the role that MMP-9 plays in psychiatric disorders and neurological processes linked with PNNs.

Memory

In the brain, long-lived proteins such as elastin and collagen (Toyama and Hetzer, 2013) are insoluble in ECM components including proteoglycans and are stabilized by their cross-linking patterns (Gogolla et al., 2009). Tsien (2013) provided evidence for the hypothesis that very long-term memories are stored as the cross-linked pattern of holes in PNNs. PNNs are also presumed to contribute to the permanence of fear memories (Gogolla et al., 2009), which are formed in the hippocampus, basolateral amygdala and lateral amygdala (Izquierdo et al., 2016) – all areas that PNNs are present in.

Addiction

Drug addiction causes remodeling activity in the brain and creates drug associated memories that drives reinforcement and addiction. Slaker et al. (2016) hypothesized that the disruption of drug- related memories by means of neuroplastic events, such as PNN induced plasticity, may lead to the suppression of relapse. The areas of the brain are associated with PNNs roles in fear-conditioned memory formation in the basolateral amygdala overlaps with drug-related memory formation. In addition, the medial prefrontal cortex and hippocampus are involved in the storage of long-term memory and fear conditioning memory (Hylin et al., 2013). In a heroin self-administration model, PNNs in the medial prefrontal cortex and nucleus accumbens of GABAergic interneurons were decreased following extinction training and forced abstinence (Van den Oever et al., 2010).

Epilepsy

Epilepsy is a chronic neurological disorder that is characterized by seizures and affecting over 70 million people worldwide. Given that PNNs mostly surround GABAergic interneurons, they are presumed to play a pivotal role in epilepsy (McRae et al., 2012). Seizures are classified as the sudden and uncontrolled electrical disturbance of the brain where nerve cell activity is disturbed. After experiencing seizures, the ECM of the brain undergoes remodeling. In the rat cortex and hippocampus, the synthesis and expression of glycosaminoglycans are altered following induced seizures (Naffah-Mazzacoratti et al., 1999). ECM remodeling also comprises the alternation of PNN density in the hippocampus following seizures. Rankin-Gee et al. (2015) reports a global loss of PNNs, as determined by WFA labeled PV+ interneurons, but also suggested that PNN digestion might lower the threshold for seizure occurrence.

Schizophrenia

Schizophrenia is a long-term mental disorder characterized by positive and negative psychotic symptoms affecting 20 million people worldwide. The onset of schizophrenia is around 20 years old (figure 2). Human subjects with schizophrenia show reductions of PNNs in the amygdala, entorhinal cortex and prefrontal cortex (Pantazopoulos et al., 2010; Berretta et al., 2015). More specifically, PNNs are more significantly distributed in the normal human amygdala but show marked decreases in the deep, lateral, basal, accessory basal, cortical, and medial amygdala nuclei of human subjects with schizophrenia (Pantazopoulos and Berretta, 2016). In all of the mentioned studies, it should be noted that the number of neurons was unchanged, only the labeled density of PNNs showed a reduction (Berretta et al., 2007; Pantazopoulos et al., 2010; Pantazopoulos and Berretta, 2016).

Alzheimer's disease

Alzheimer's disease is a progressive neurodegenerative disease that destroys memory and other mental functions. Characteristic to Alzheimer's disease is the formation of β-amyloid plaques. Heparan sulfate proteoglycans and chondroitin sulfate proteoglycans are implicated in the formation of β-amyloid plaques (Bruinsma et al., 2009) and postmortem brains of subjects with Alzheimer's disease have been reported with high levels of heparan sulfate proteoglycans, compared to the normal brain. WFA-labeled PNNs density is reportedly decreased in Alzheimer's disease, specifically in the frontal cortex and in the entorhinal cortex of postmortem brains (Baig et al., 2005).

Another protein implicated in Alzheimer's disease are misfolded tau proteins, which form tau tangles. Interestingly, Morawski et al. (2010) reported that aggrecan-based PNNs plays a protective role against tau protein pathology in Alzheimer's disease, supporting a neuroprotective role of PNNs in the cortex.

Brain and spinal cord injury

In cases of spinal cord injury, neuronal remodeling occurs to compensate for the injury. Following dorsal spinal cord injury in rats, and subsequent task-specific rehabilitation in combination with ChABC degradation, PNN density and staining intensity were shown to increase (Wang et al., 2011). Thus, ChABC degradation of PNNs promotes brain plasticity (Fawcett et al., 2019).

Stroke and other nervous system injuries induces axonal sprouting and peripheral nervous system regeneration, however, to a limited extent. In a stroke model in the rodent barrel cortex (Carmichael et al., 2005), the expression levels of neuroncan, phosphocan, versican, brevican,

and aggrecan are increased in a time course specific manner but, PNNs are reduced following stroke in the peri-infarct cortex after day three and then increase again post stroke day 28, although the original laminar pattern is not fully recovered. In another experimentally induced ischemic stroke model, PNNs were drastically reduced one day following ischemia onset in the nucleus reticularis thalami (Hartig et al., 2016).

PNNs are altered in many neuronal pathologies. In neuropsychiatric patients diagnosed with major depression, bipolar disorder or schizophrenia, the PNN density is lower in those patients compared to controls (Alcaide et al., 2019). However, it is still an open question whether those changes in the PNN is a result of the pathology (response) or if their misfunction leads to the pathology itself – or both.

Chapter 3: The Barrel Cortex

PNNs are expressed in multiple anatomical regions, including in the rodent barrel cortex (Zimmermann and Zimmermann, 2008; McRae et al., 2007). In the primary somatosensory (S1) cortex, each whisker on the snout of the rodent is represented by a discrete "barrel" structure within the contralateral layer IV of the rodent's brain together known as the barrel cortex (Woolsey and Van der Loos, 1970; Peterson, 2007). The whiskers on the snouts of rodents serves as sensitive detectors for acquiring information about the environment and functions in fine-grain texture discrimination (Brecht, 2007), and the barrels in the cortex are responsible for processing tactile information. Synaptogenesis in the somatosensory cortex of glutamatergic and GABAergic synapses is fundamental for the development of social behaviors, such as huddling (Naskar et al., 2019).

By the end of the first week of life, excitatory and inhibitory neurons migrate from the deep to superficial layers of S1 **(**Naskar et al., 2019). Sensory information from the whiskers are transmitted to the thalamus and thalamocortical fibers of the thalamus projects to layer IV of S1. From layer IV, these fibers projects to other layers and then to further cortical regions. In early post-natal life, the thalamocortical pathways of the rodent barrel cortex is deemed "plastic" (Fox, 2002) but by one to two months of age, plasticity decreases and the intracortical pathways becomes more important thereby restricting the temporal window of plasticity. The rodent barrel cortex is ideal for studying mechanisms of brain plasticity since plasticity can be induced by whisker deprivation. Unilateral whisker trimming within the first month of post-natal life leads to a significant reduction of PNN expression in the mouse barrel cortex (McRae et al., 2007).

3.1 Laminar Distribution

There are six layers of the barrel cortex: layers I, II/III, IV, V and VI. PNNs are present in all layers, but PNN expression is uneven between layers. PNNs are enriched in layers IV and V of the barrel cortex with the highest levels of expression in layer IV (Lipachev et al., 2019; McRae et al, 2007). PNNs are present in lesser extent in layers I, II/III, and VI.

Aim of Study

In this study, we aim to give a comprehensive picture of PNN expression throughout the cortex by looking at over 20 different anatomical regions throughout the adult Long Evans rat brain. Previous studies have only analyzed PNNs expression in selected cortical regions in smaller scales. In addition, we aim to look at the density of PNNs between the layers of the barrel cortex.

Chapter 4: Materials and Methods

4.1 Animals

Experiments were performed on male Long Evans rats (N=7), approximately 3 months of age and weighing between 300-400 grams. All rats were individually housed under a reverse 12-hour light/ 12-hour dark cycle. All rats had unlimited access to Purina rat chow and water at all times. All experimental procedures followed the protocols approved by the Institutional Animal Care and Use Committee of Queens College, CUNY (Protocol #120) and were consistent with NIH guidelines for responsible use of animals in research.

4.2 Histochemistry

Rats were anaesthetized with 3mL Euthasol (Euthanasia Solution, Virbac Animal Health) administered via intraperitoneal injection. Immediately after becoming unresponsive to a noxious stimulus (toe pinch) all animals were perfused intracardially with a 0.01M phosphate buffer saline (PBS, pH 7.4) followed by ice cold 4% paraformaldehyde (pH 7.4) dissolved in 0.1M PBS. Brains were extracted and postfixed in 4% paraformaldehyde dissolved in 0.1M PBS overnight at +4°C. Fixed brains were sectioned coronally rostral to caudal at 60µm in 0.01M PBS using a vibratome (Leica Vt 1000s). Using the Paxinos and Watson Atlas (2007) three sections were selected for histochemistry: an anterior section (approximately 3.24mm anterior relative to bregma), middle (approximately 1.20mm relative to bregma), and a posterior section (approximately -2.64mm relative to bregma). These sections were selected to give us a wide range of cortical regions, including the barrel cortex in the middle section. Selected slices were washed in 0.01M PBS three times, 10 minutes each on an orbital shaker. To stain for PNNs, we used conjugated *Wisteria floribunda* agglutinin, (WFA, Vector Laboratories, catalog no. FL-

1351) and the cellular stain, Hoechst (Hoechst 333423, Molecular Probes, catalog no. H-1399), 0.12µg/ml. Slices were incubated in WFA and Hoechst for 2.5 hours on an orbital shaker at room temperature. Slices were then washed in 0.01M PBS three times, 10 minutes each on an orbital shaker. Fluorescently stained sections were submerged in distilled water and then mounted onto a 24x40mm glass subbed slides and allowed to air dry overnight. The next day, dried slices were cover slipped with anti-fade mounting medium (Vector Laboratories) and allowed to dry overnight prior to examination under the microscope.

4.3 Microscopy Imaging and Data Analysis

All images were obtained using an Olympus BX51 microscope (Olympus America Inc., Melville, NY, USA) using the DAPI (excitation wavelength (Ex):405 emission wavelength (Em):461) and FITC (Ex: 473 Em:519) filters. Using Neurolucida 7.5 software (MBF Bioscience), either the left or right hemisphere was contoured under DAPI at 4x (numerical aperture (NA) = 0.10). Camera settings were held constant with exposure ~ 1ms, contrast =59, brightness =55, and gamma =0.917. After the entire hemisphere was contoured, the filter and the objective were switched to FITC and 10x (NA = 0.25) to get a higher magnification image of the selected hemisphere. An arbitrary reference point was selected in order to acquire virtual tissue. The virtual tissue module is used to acquire two dimensional (2D) high-resolution images on a single plane in which individual images are acquired and then merged to form a virtual slide. All images were saved as a 2D JPEG2000 file with a compression ratio of 5:1 to reduce the size of the resultant image files. In order to capture a complete hemisphere a total of 50-80 images were consecutively acquired depending on need (**figure 3A, B**).

4.4 Quantification and Analysis of PNNs

PNNs were manually marked and counted in Neurolucida 11.01 (MBF Biosciences). Classification of PNNs includes a clearly labeled soma and proximal dendrites (**figure 3C, D)**. PNNs were not marked if the diameter of their associated soma was under 9 μm in order to provide a consistent measure of the PNNs. The quick measure circle tool and quick measure line tool on Neurolucida was used to estimate the diameter of ensheathed neurons (**figure 4**). Using the Paxinos and Watson (2007) atlas as reference, cortical regions were contoured (**figure 3B**). Neurolucida files with identified cells ensheathed by PNNs and contours or cortical areas were saved and opened in Neurolucida Explorer to extract PNN counted markers and area per contoured regions. PNN density was calculated by dividing PNN count by the enclosed contour area. Cortical laminae were based on cell density/size as revealed by Hoechst staining (**figure 3C**) and WFA (**figure 5**). Luminance measure of brightness was recorded among layers of the barrel cortex and white matter for comparison (**figure 5**) a luminance correction was applied by normalizing cortical brightness of a specific lamina by that lamina's cross-sectional area (**figure 5**).

Graphs and ANOVAs were created in SigmaPlot 10.0. Kruskal-Wallis one-way analysis of variance on ranks and all pairwise multiple comparison procedures (Tukey's test and Dunn's method) were conducted.

Random Effects Model

To better understand the relationship between cortical area and PNN density we constructed the following random effects model. The model summarizes PNN density as a function of regions and subjects (assuming no other confounding variables), where data is drawn

from the population of regions and population of subjects. It enabled an estimation of the variance components, i.e., variability explained by regions, variability explained by subjects, and the variability not explained (residual / error), and whether a variance component is statistically significant. Adjusting for individual subject essentially implies differences among rats—including physiological, genetic or other differences —which are accounted in the model. Total sample size n=658, with 34 regions of a brain and 7 mice.

Equation 1:

$$p_{ij} = \mu + r_i + s_j + \varepsilon_{ij}$$
$$r_i \sim iid\ N(0, \sigma_r^2)$$
$$s_j \sim iid\ N(0, \sigma_j^2)$$
$$\varepsilon_{ij} \sim iid\ N(0, \sigma_\varepsilon^2)$$

$i = 1, \dots, 34\ regions$
$j = 1, \dots, 7\ subjects\ (rats)$

$p_{ij} =\ PNN\ density\ in\ region\ i\ sampled\ from\ subject\ j$
$\mu = overall\ mean\ of\ all\ regions\ (intercept;\ grand\ mean; fixed\ effect)$
$r_i = intercept\ of\ region\ i\ (random\ effect)$
$s_j = intercept\ of\ subject\ j\ (mice;\ random\ effect)$
$\varepsilon_{ij} = residual\ (errors; random\ effect)$

$\sigma_r^2 = variance\ attributed\ to\ regions$
$\sigma_s^2 = variance\ attributed\ to\ subjects$
$\sigma_\varepsilon^2 = variance\ attributed\ to\ errors$

Using SAS (Cary, NC) on a PC the Proc Mixed procedure was utilized to implement our model.

Chapter 5: Results

5.1 Areal Differences in PNN Density

PNNs were visualized throughout the brain as brightly stained structural outlines of the neurons that they surround (**figure 3D, figure 4**). WFA staining revealed neuronal somata surrounded by PNNs that visually varied in their density as a function of cortical area and lamina. As previously reported, WFA staining only targets the soma and the proximal dendrites (**figure 4B**). We quantified the number of PNNs at three different coronal locations in the rat brain: anterior (bregma +3.24mm), middle (bregma +1.20mm), and posterior (bregma -2.64mm), thereby analyzing 26 different cortical regions throughout the rostral-caudal extent of the rat neocortex (**figure 6, table 1**). The mean PNN density throughout the cortex was 0.41 +/- 0.05 PNNs/mm^2 (data represent populations means +/- one standard error of the mean). As is apparent from **figure 6** there were significant regional differences in PNN density. Kruskal-Wallis One Way Analysis of Variance on Ranks revealed that the differences in the median values among cortical regions were greater than what would be expected by chance ($p < 0.001$). In addition, utilizing the random effects model (**equation 1**) allowed us to efficiently analyze the variance components and conclude that the variability explained by regions were statistically significant. The motivation of utilizing this methodology was to prevent errors in assigning significance to interactions between cortical areas which can happen if multiple paired comparisons were done.

Subsequent pairwise comparisons using Dunn's Method also showed significant differences ($p<0.05$) between distinct cortical regions (**figure 6**). The caudal retrosplenial granular cortex (RSGc) and retrospenial dysgranular cortex (RSD) had the highest PNN density, accordingly. Following in descending order are: frontal cortex area 3 (Fr3), granular insular cortex (GI) and the primary somatosensory cortex (S1), cingulate cortex area 2 (Cg2), and

secondary somatosensory cortex (S2). The intermediate endopiriform nucleus (IEn) had the lowest PNN density.

Figure 6A displays the PNN density as a function of brain region. While it is apparent upon visual inspection that different brain regions possessed unique PNN densities we wanted to better understand the nature of their distribution which are shown in **figure 6B.** Based on the random effects model detailed in the methods section we observed that cortical region ($p < 0.0001$) and subject ($p < 0.0448$) are both significant predictors of protein density, subsequent analysis revealed that cortical region accounted for approximately 60% of the variance within our data set. This analysis provides statistical support that PNN expression varies as a function of cortical region.

5.2 Motor versus Somatosensory Cortex

The primary motor and somatosensory cortices' in rodents are highly adaptable to their function of exploration and interaction with the external environment due to their prominent facial whiskers (Peterson, 2007; McRae et al, 2007). Thus, we focused our comparisons on those two areas. The primary somatosensory cortex had significantly higher levels of PNNs then the primary motor cortex ($p = 0.002$, **figure 7A**). To test whether a lateralization effect existed we compared the PNN density between the two hemispheres (**figure 7B**). The right hemisphere of both M1 and S1 had a slightly higher PNN density compared to the left, but the differences did not reach statistical significance for either cortical area ($p's > 0.05$).

Next, to determine whether PNN density was consistent across a given cortical region we focused on S1. Based on the somatotopy of S1, it can be divided into seven sub regions: jaw region (S1J), forelimb (S1FL), dysgranular (S1DZ), oral dysgranular (S1DZO), upper lip (S1Ulp), trunk regions (S1Tr), and barrel field (S1BF). A comparison of the PNN densities

within each subregion of S1 did not reveal any difference between (p's>.05), thus the density of PNNs were consistent across S1 (**figure 8A**).

5.3 Laminar Analysis

Continuing with our focus on S1, we quantified PNN densities based on laminar distribution of the barrel cortex. Our results demonstrated that similar to those observed mice (Nowicka et al., 2009), layer IV of the barrel cortex in the Long Evans rats displayed the highest PNN density. Layers V, II/III, and VI followed in descending order (**figure 8B**). The density of PNNs in layer 4 was significantly higher than those observed in layer I, II/III, and VI ($p < 0.05$); the PNN density in layer V was significantly higher than those observed in layer I and VI ($p<0.05$); and layer II/III had a higher density of PNNs then layer I ($p<0.05$). Thus, PNN density is not uniform within a cortical column but varies as a function of cortical depth with layer IV exhibiting highest PNN density.

5.4 Deep Layer Staining

Consistent across all animals (n=7) and in virtually every slice, we observed brightly stained PNNs surrounding neurons in deep layer VI along the border of the white matter (**figure 9A, B**). The role that these cells specifically play are unknown**.** Layer 6 consists of a diverse population of neurons with specific sub laminar organizations and distinct morphologies and thus these cells may represent a phenotype unique to layer 6 (Zhang and Deschenes, 1997, 1998; Chen et al. 2009; Zarrinpar and Callaway, 2006). Typical WFA+ cells (n=30) found in proximity to the brightly labeled neurons in layer 6 had a mean diameter of 12.96 +/- 0.29 μm whereas the larger, bright WFA+ cells (n=30) had an average diameter of 20.46 +/- 0.46 μm. Comparing the typical cells versus the large cells, revealed that the larger cells possessed significantly greater

diameters (t-test, $p < 0.001$). Based on the obvious size and greater distance between these cells, we quantified the distance between typical WFA+ neurons and large WFA+ cells (**figure 9C).** On average, the typical cells (n=102) were closer together with a soma center-to-center average distance of 73.7 +/- 4.2 μm while the large WFA+ cells (n=93) had a statistically larger (t-test, $p<0.001$) average separation distance of 306.8 ± 49.5 μm from their neighboring large cells in layer VI.

Chapter 6: Discussion

6.1 Summary

Our investigation revealed that PNN density was not uniform across the rat cortex, with variance as a function of both area and lamina. PNN density was slightly higher in the right hemispheres of S1 and M1 compared to left hemisphere, but not to statistical significance. Lau et al., 2020 showed a similar trend and reaching statistical significance between hemispheres. The relative densities of PNNs found in the distinct cortical regions may be reflective of the ease or difficulty of inducing plasticity in those cortical regions.

In primates, PNNs are associated with distinct populations of non-cholinergic neurons in the basal forebrain nuclei and absent around the cholinergic basal forebrain neurons (Adams et al., 2001). A region-specific pattern of PNN distribution has also been demonstrated previously in mammals such as rats and raccoons. In the rat, basal forebrain PNNs were shown to display selective distributions for certain neuronal populations (Brauer et al., 1993). Further evidence of region-specific PNN distribution in the rat basal forebrain revealed PNNs localization in certain basal forebrain subdivision such as the septal-diagonal band region but only scarcely present in the ventral pallidum (Brauer et al.,1995). In raccoons (Brauer et al., 1999), noncholinergic neurons of the medial septum and lateral septum were surrounded by PNNs while the cholinergic cells of the medial septum were not. Hagihara et al. (1999) revealed that PNNs and its component tenascin-R and brevican shared similar distribution patterns in regions such as the reticular formation, deep cerebellar nuclei, the red nucleus and the gigantocellular nucleus of the adult rat. Consistent with our findings, regional variations in the cortex have also been shown in rats previously (Seeger et al., 1994).

In another recent study, Beebe et al (2017) investigated PNN distribution in the subcortical auditory system of the Guinea pig, mouse, Long-Evans rat, and the naked mole-rat. While PNN distribution is similar across species in the ventral and central cochlear nuclei, they varied in the dorsal cochlear nucleus. Beebe et al (2017) also found that PNNs were expressed in the vestibular nuclei, red nucleus, and the reticular formation across species and mainly deficient in the medial geniculate body.

Lensjo et al (2017) examined the visual cortex, hippocampus and the medial entorhinal cortex and reveled that PNN density and laminar distribution were different across these brain regions. Of the cornu Ammonis regions of the dorsal hippocampus; PNNs were intensely expressed in CA2, moderately expressed in CA3 and minimally expressed in CA1. The superficial layers of the medial entorhinal cortex densely expressed PNNs while the deeper layers expressed very few PNNs.

Hausen et al., 1996 reported PNNs predominately in layers II-IV of human motor area 4, as well as in somatosensory areas 1-3. PNNs surrounding pyramidal neurons were predominately in layers III and V in the precentral motor and postcentral somatosensory areas, further supporting the area-specific peculiarities of PNN in the cerebral cortex and distinct from what we observed in rats which had the highest density of staining in layer IV.

Interestingly, it has been shown that different cortical regions have different thresholds for the induction of synaptic potentiation or depression (Bliss and Cooke, 2011). In areas such as the perirhinal cortex, the removal of PNNs results in increased long-term depression and increased synaptic transmission (Romberg et al., 2013).

6.2 PNN Localization

In our present study, the RSGc and RSD had the highest levels of PNNs. The retrosplenial cortex is one of the largest cortical areas in the rat brain and it plays a key role in the processing of spatial information and memory (Czajowsky et al., 2014; Katche et al., 2017). Consistent with other studies, layer IV of the barrel cortex had high levels of PNN expression (McRae et al. 2007). Plasticity is difficult to induce in layer IV in adults (Crair and Malenka 1995) and higher density of PNNs in layer IV may act to crystalize the network and prevent aberrant forms of plasticity.

6.3 Sub-plate Neurons and Plasticity

Sub-plate neurons have been hypothesized to play a role in regulating critical period plasticity within the cortex (Kanold, 2004). In the visual cortex, Kanold et al. (2003) showed that the ablation of sub-plate neurons prevents ocular dominance column formation in the cat visual cortex, suggesting that the sub-plate circuits are necessary for synaptic remodeling and maturation in the cat visual cortex.

In rats, sub-plate neuron birth begins at embryonic day 12-15 (Bayer et al., 1990) and sub-plate death by apoptosis occurs from embryonic day 20-30 (Al-Ghoul, 1989; Ferrer, 1990; Wang et al., 2010) although we were able to see PNN ensheathing sub-plate neurons in the adult rat. It is not clear whether the “large” WFA+ cells we observed in the deep layers of the cortex are indeed remnants of subplate neurons although we have previously identified similarly large neurons in a Golgi study of layer 6 in the mouse (Chen et al. 2009). Considering the role of PNNs in regulating plasticity (Tsien 2013), it is possible that the brightly stained PNN ensheathing neurons which we observed may play a role in regulating plasticity in the cortex.

Although there are similarities in the subplate genetic expression patterns between humans and rodent models, unlike rodents- humans have a larger zone for cellular organization for these cell types (Wang et al., 2010). In a human study, sub-plate neuronal injury was suggested as a likely cause of perinatal brain injuries which results in specific neurodevelopmental defects (McQuilen and Ferriero, 2005). It is possible that at term gestational sub-plate neuronal injuries can interfere with the critical period considering that the human sub-plate development is highest when thalamocortical connections are formed and influenced by the activity-dependent critical period.

6.4 PNNs Clinical Implications

Ultimately, a better understanding of PNNs and the effects of their presence or absence in specific cortical regions in the brain may lead to therapies for a variety of CNS pathologies. PNNs have been shown to be altered in schizophrenia (Berretta et al., 2015) in both mouse models and in the mPFC of human subjects (Mauney et al., 2013). The densities of PNNs in human postmortem brains decreased significantly in the layers 3 and 5 of PFC in cases of schizophrenia (Mauney et al., 2013). Given PNNs preference to ensheathe GABAergic interneurons it follows that they may play a role in regulating the progression of epilepsy (Berretta et al., 2015). PNN dysfunction has been also observed in human Alzheimer's disease (Miyata et al., 2007; Morawski et al., 2012); strokes and other CNS injuries (Bradbury et al., 2011). In the absence of PNNs it is assumed that neurons of the cholinergic basal nucleus are more exposed to injury, manifesting in degenerative diseases such as Alzheimer’s disease (Adams et al., 2001). Further, recent research has shown that altered PNN formation during development may produce synaptic changes associated with the clinical brain disorders of bipolar disorder, major depression, and autism (Folsom and Fatemi, 2013; Sorg et al., 2016).

Thus, understanding the distribution of PNNs is a necessary first step to hypothesizing their potential role in normal and pathological brain states and may offer insights into new treatment approaches for these pathologies.

6.5 Limitations

Collecting data such as what is contained in this study is time consuming, hence, we have limited samples per region. Small sample size per region (n=14 in most regions, some 28, 42) which could be a problem in ensuring a representative population. Each brain region has millions of cells, so collecting 14 cells may not reflect the population level distribution, and it is possible that we may have missed some values, not within the range of our boxplot for a region. Hence, these effects (region means) may change if another study is conducted, so we need replication of this study to estimate the true effect (mean) of a region. That being said, other studies using similar methodologies have also found regional differences in PNN density (Fader et al., 2016; Lensjo et al., 2017), which suggests that this finding is robust.

Another limitation of this study is that only male adult rats were used. Given that this is a naive study and no sex differences were expected, we did not require sex as a criterion in subject selection. We recognize that sex bias is an issue and will incorporate both genders in future studies.

6.6 Concluding Remarks

In this study we aimed to characterize PNN density throughout the adult rat brain and we were successfully able to look at 26 different cortical regions and the barrel field. Given the prominent role of the rodent's whiskers and its function to largely compensate for poor vision, it was not surprising that the somatosensory cortex had a high PNN density. Interestingly, the

retrosplenial granular cortex and the retrosplenial dysgranular cortex had the highest density of PNNs. The rat retrosplenial cortex (RSC) consists of the dysgranular region: especially important for spatial memory, and the granular region: involved in navigation (Pothuizen et al., 2009; Vann et al., 2009; Yamawaki et al., 2016). The RSC circuit connects the anterior thalamic nuclei, the lateral dorsal thalamic nucleus and the hippocampus **(**Van Groen et al., 2003; Vann et al., 2009; Yamawaki et al., 2016). Interestingly, Yamawaki et al., (2016) showed a direct corticocortical link between the retrosplenial cortex and M2 in the mouse, suggesting functional connections of projecting neurons between the two regions. Additionally, the RSC is also involved in episodic memory (Yamawaki et al., 2016) and a major factor in the storage of memories is cortical plasticity (Katche et al., 2017). The anterior retrosplenial cortex plays a critical role in fear memory consolidation, both recent and remote (Yamawaki et al., 2016)

Ultimately a better understanding of PNNs and the effects of their presence or absence in specific cortical regions in the brain can lead to therapies for plasticity and CNS pathological conditions. PNNs has established clinical implications in cases of schizophrenia in rodents and humans (Berretta et al., 2015; Mauney et al., 2013); in clinical implications revolving around synaptic stability in the progression of epilepsy (Berretta et al., 2015); association with the amyloid plaques in human Alzheimer's disease (Miyata et al., 2007; Morawski et al., 2012), for CSPG modification in stroke and other CNS injuries (Bradbury et al., 2011); in terms of long term memories (Tsien, 2013) and enhancement of memory when PNNs are degraded or by genetic deletion (Romberg, 2013); as well as in cases of drug addiction (Slaker et al.,2016; Van den Oever et al., 2010). Given the importance of PNNs in so many human pathological disorders, any contribution to the understanding of PNNs in the brain holds potential for getting one step closer to therapeutic approaches.

Figures

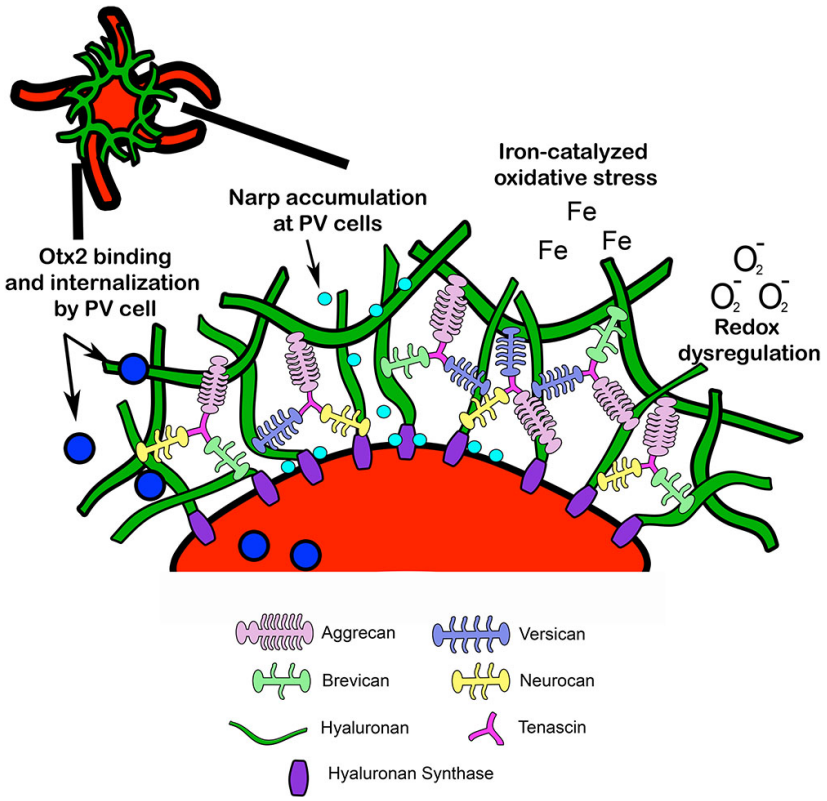

Figure 1. Structural composition of PNN.

Structural composition of PNN. Lecticans are attached to a hyaluronan backbone via link proteins such as cartilage link protein and hyaluronan link proteins (not pictured). Hyaluronan synthase contributes to hyaluronan synthesis and anchors hyaluronan to the cell membrane. Tenascin promotes crosslinking of lecticans and helps maintain PNN structural integrity. PNN around PV cells may provide protection from redox dysregulation and oxidative stressors such as superoxide free radicals (O_2^-) and metal ions (Fe). In addition, PNNs may facilitate PV maturation through internalization of Otx2 homeoproteins and regulate PV cell excitability through accumulation of the immediate early gene and synaptic scaling molecule Narp. Narp, neuronal activity-regulated pentraxin; Otx2, orthodenticle homeoprotein 2. *Adapted from Wen et el., 2018.*

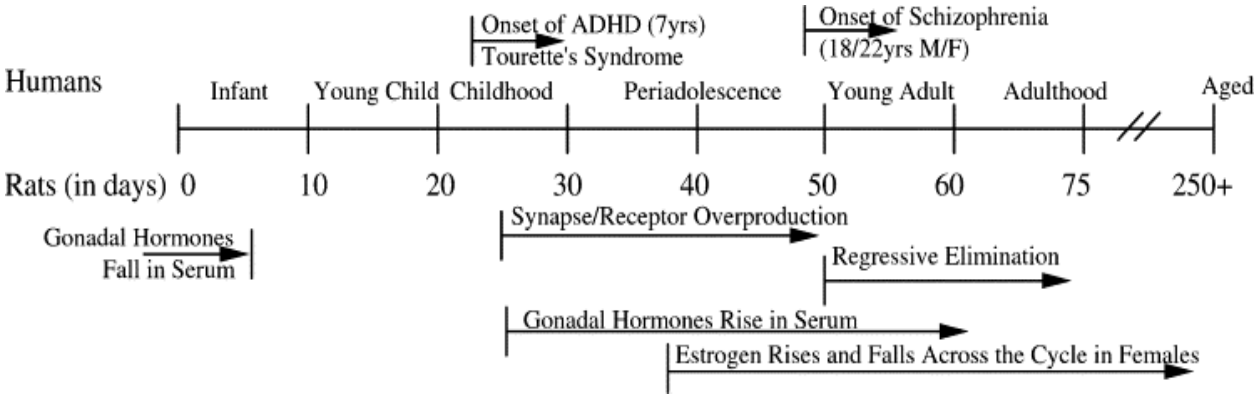

Figure 2. A relative comparison of ages and stages of human versus rat development. Juvenile mice (P28–35) corresponding to adolescence. Onset of ADHA and Tourette's Syndrome beginning at around 7 years in human children and corresponding to day 21 in rats. The onset of schizophrenia beginning around 18 years in human males and 22 years in females corresponds to day 48 in rats. Similar patterns of synapse and receptor overproduction and regressive elimination are present in corresponding life points between humans and rats. *Adapted from Andersen, 2003.*

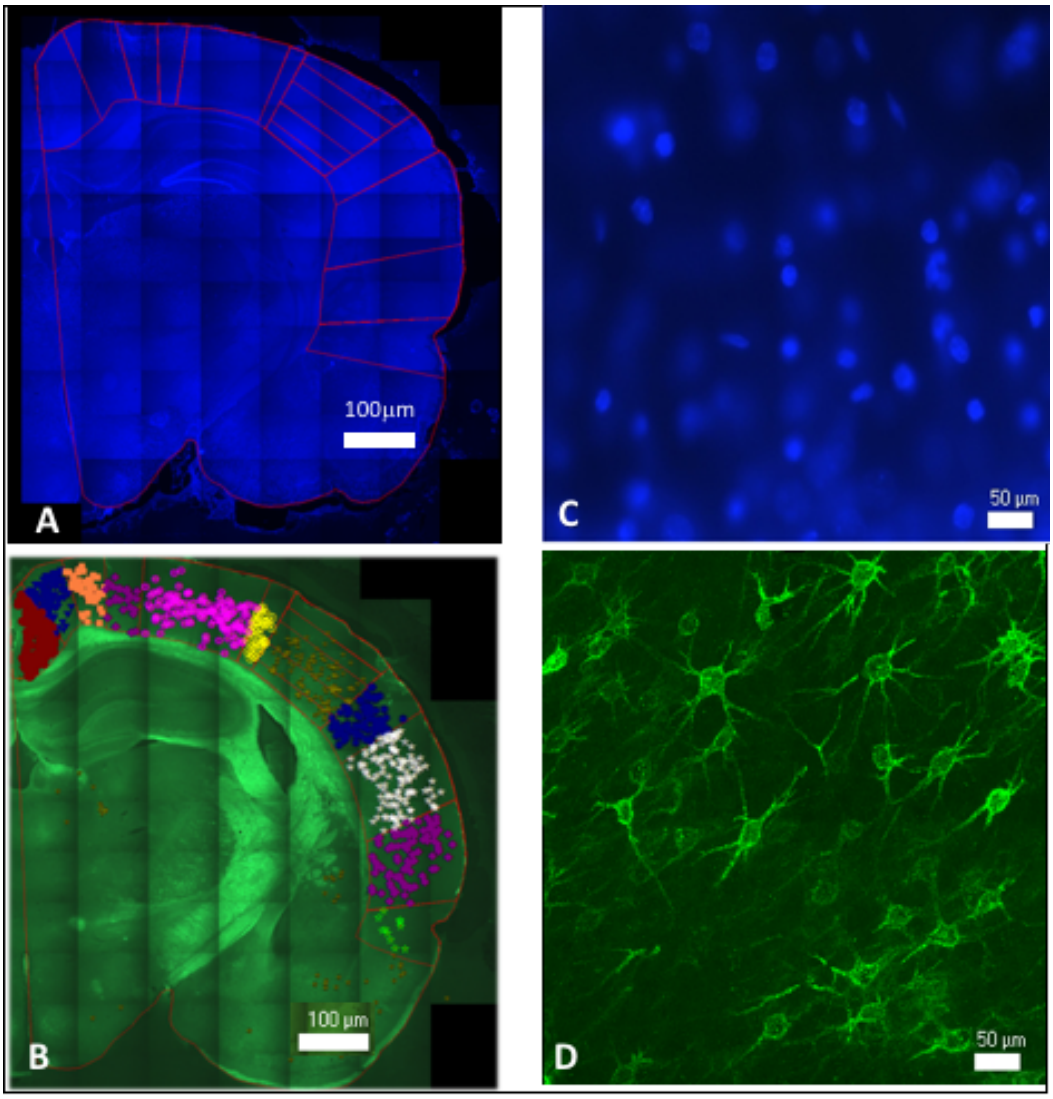

Figure 3. Methodology

(A) Whole hemisphere florescent image acquired via virtual slice module and then 'stiched' together, Hoechst. (B) Selected cortical regions contoured (red) using the Paxinos and Watson atlas (2007) as reference, WFA. (C) 60x magnification showing neuronal nuclei, Hoechst. (D) High magnification of PNN, WFA.

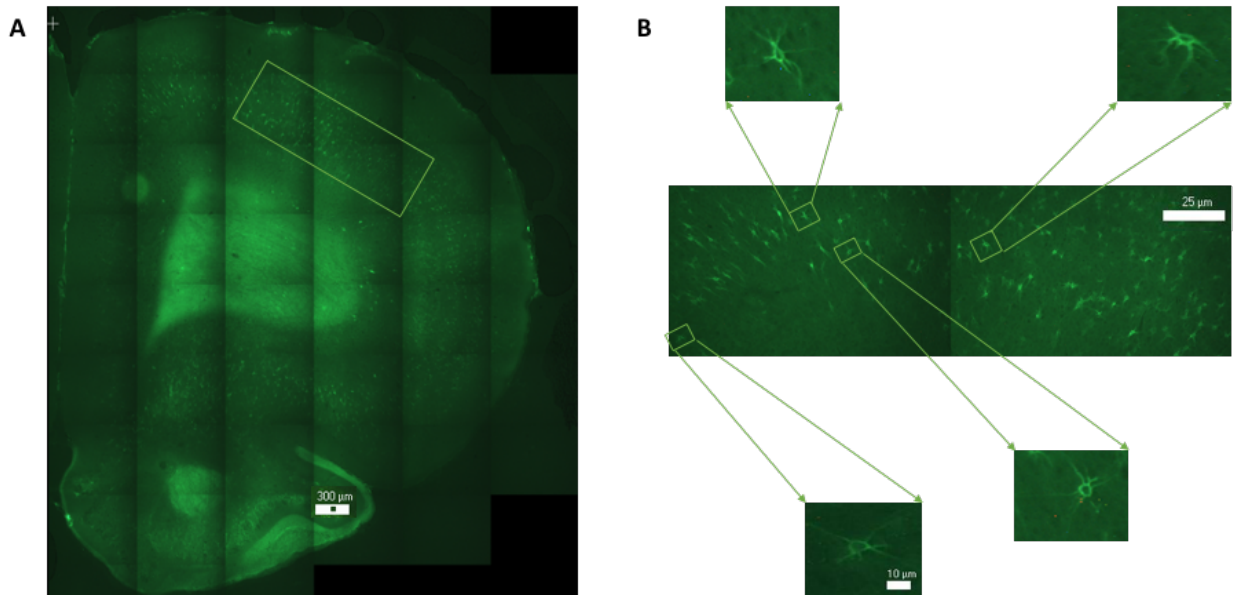

Figure 4. Perineuronal nets (PNNs) revealed with fluorescent WFA staining.

(A) Right hemisphere of adult male Long Evans rat shown, PNNs labeled with WFA. (B) PNN lattice-like structures ensheathing somata, proximal dendrites and axons. All inset images taken at the same magnification.

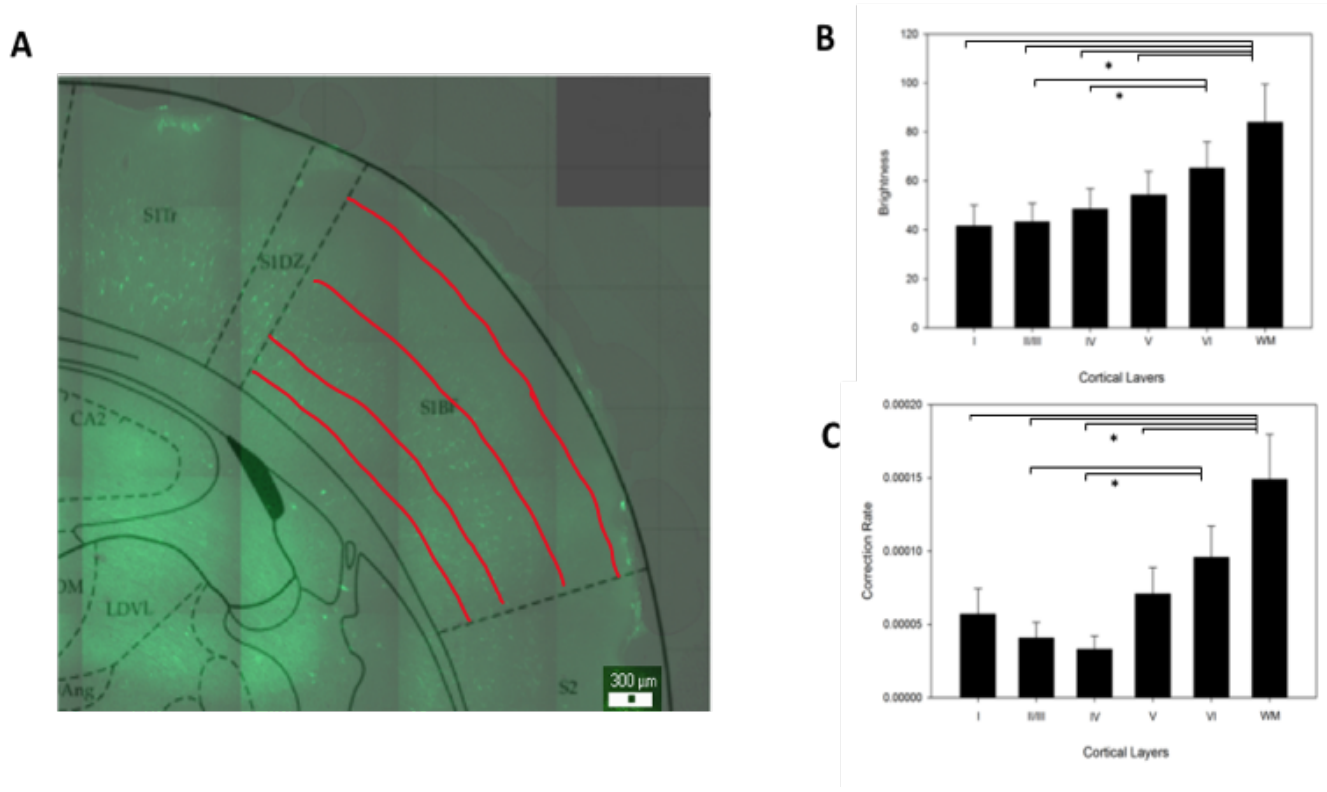

Figure 5. Brightness and luminance correction rate.

(A) Contour makers of S1 barrel field in posterior coronal section, 10x magnification. Layers I, II/III, IV, V, VI, and white matter (WM) contoured. (B) Luminance measure of brightness among layers of barrel cortex and WM. The differences in the median values among the layers are greater than would be expected by chance; there is a statistically significant difference (P = <0.001). Significance between WM vs layers I, II/II, IV, V and VI vs I, II/II. (C) Luminance correction rate (brightness/area). All Pairwise Multiple Comparison Procedures (Tukey Test) revealed statistical significance (P<0.05) between WM vs layers I, II/III, IV, V and VI vs IV, II/III. Brightness and correction rates are measured with respect to cortical layers. WFA luminance correction rate = brightness/ μm^2.

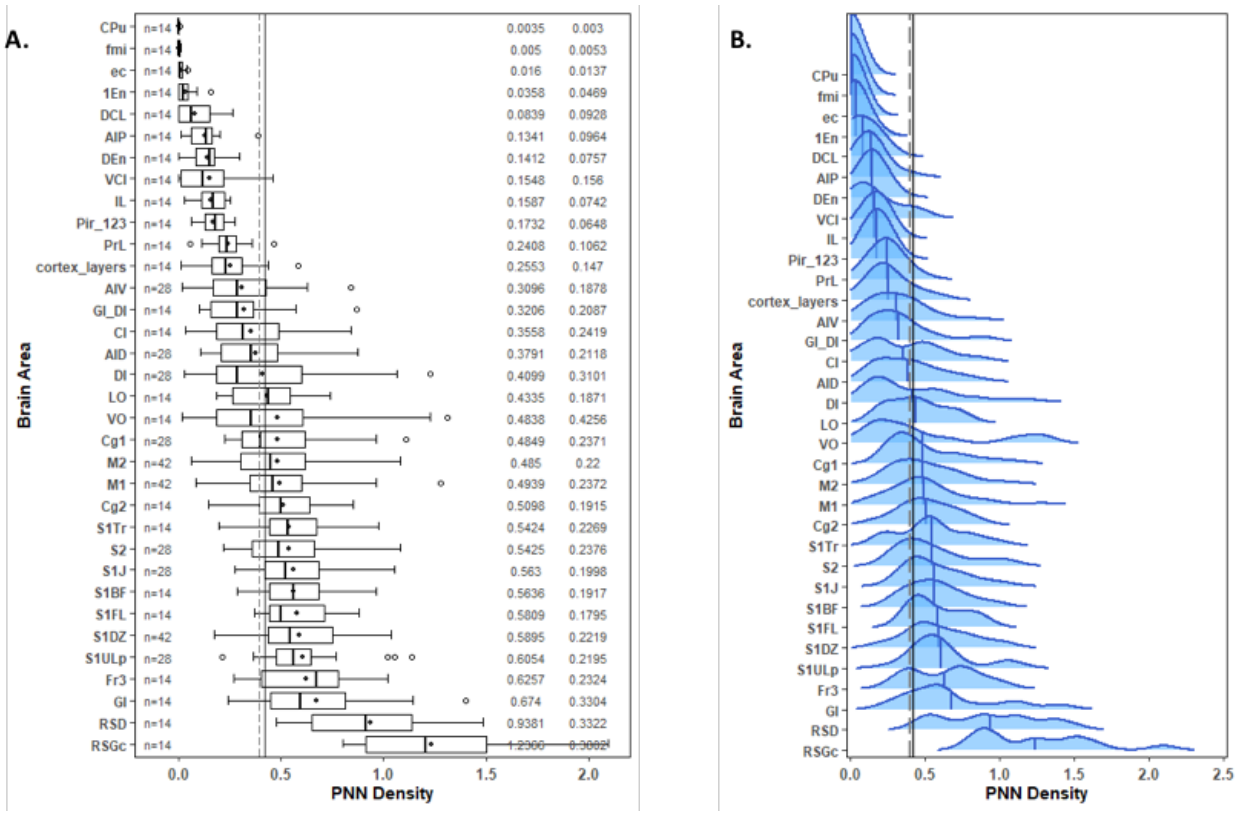

Figure 6. Whole Brain PNN Density.

PNN density in 26 different cortical regions of the Long Evans rat brain. (A) box plot of brain areas and PNN density. (B) Kernel density plot. Cingulate cortex area 2(Cg2), secondary motor cortex (M2), primary motor cortex (M1), secondary somatosensory cortex (S2), primary somatosensory cortex (S1), frontal cortex area 3 (Fr3), lateral orbital cortex (LO), granular insular cortex (GI), retrosplenial granular cortex c (RSGc), and retrosplenial dysgranular cortex (RSD) had means higher than population means, as determined by one-way ANOVA. The first quartile represents 25 percentiles of which the data are below, and third quartile represents 75th percentile. All outliers are shown (black dots).

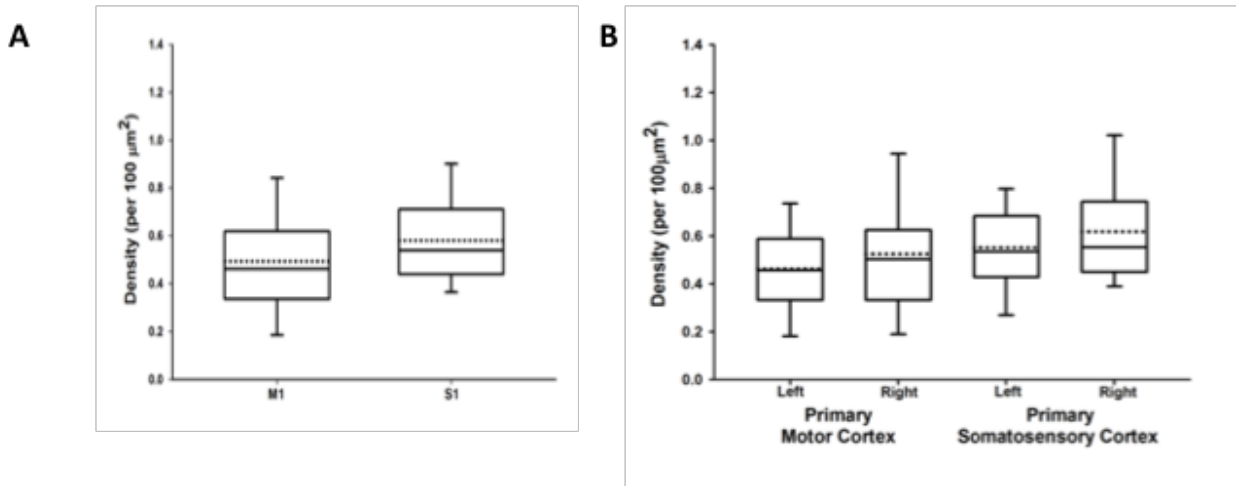

Figure 7. PNN Density in Motor Cortex vs Somatosensory Cortex

(A) Box and whiskers plot of PNN density in M1 and S1. The top horizontal line of the box represents the third quartile and the bottom horizontal line represents the first quartile. Solid line represents median, dotted line represents mean value of PNN density of the respected region. There is a statistically significant difference between PNN density in the motor cortex (M1) and somatosensory cortex (S1). S1 has a significantly higher PNN density ($p = 0.002$) compared to M1. (B) PNN Lateralization in M1 and S1. There is not a statistically significant difference of PNN density in M1 or S1 between the left or right hemispheres.

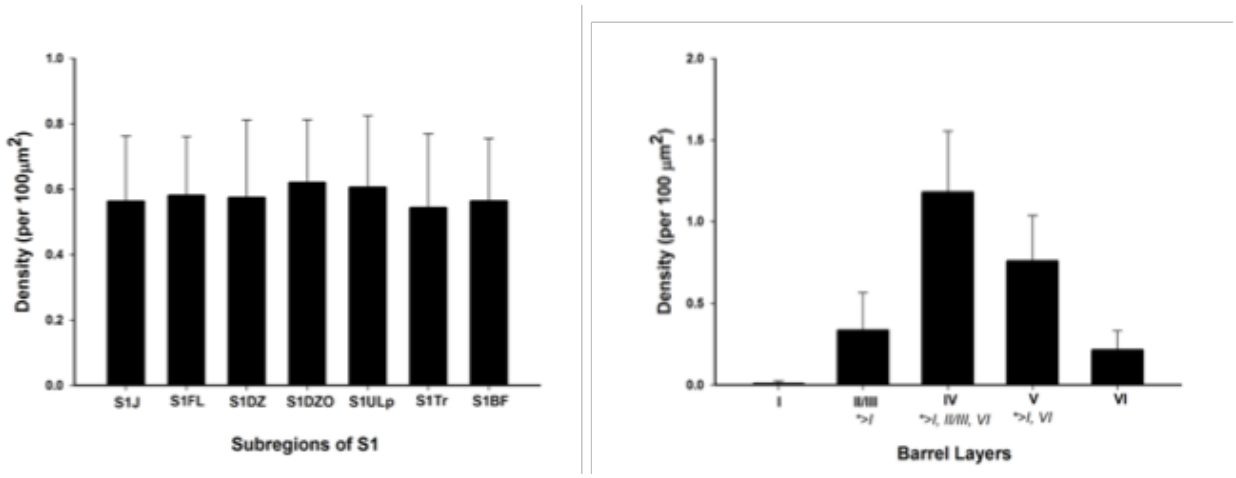

Figure 8. PNN Density in the primary somatosensory cortex.

(A) PNN Density in S1 Sub-Regions. Jaw region (S1J), forelimb (S1FL), dysgranular (S1DZ), oral dysgranular (S1DZO), upper lip (S1Ulp), trunk regions (S1Tr), barrel field (S1BF). There is no significant differences among S1 subregions ($p = 0.951$). (B) PNN Density in Barrel Field varies by cortical lamina. Pairwise comparisons that were statistically significant are indicated below the x-axis. Bars in A and B represents PNN density means$\pm$ one standard error of the mean (SEM).

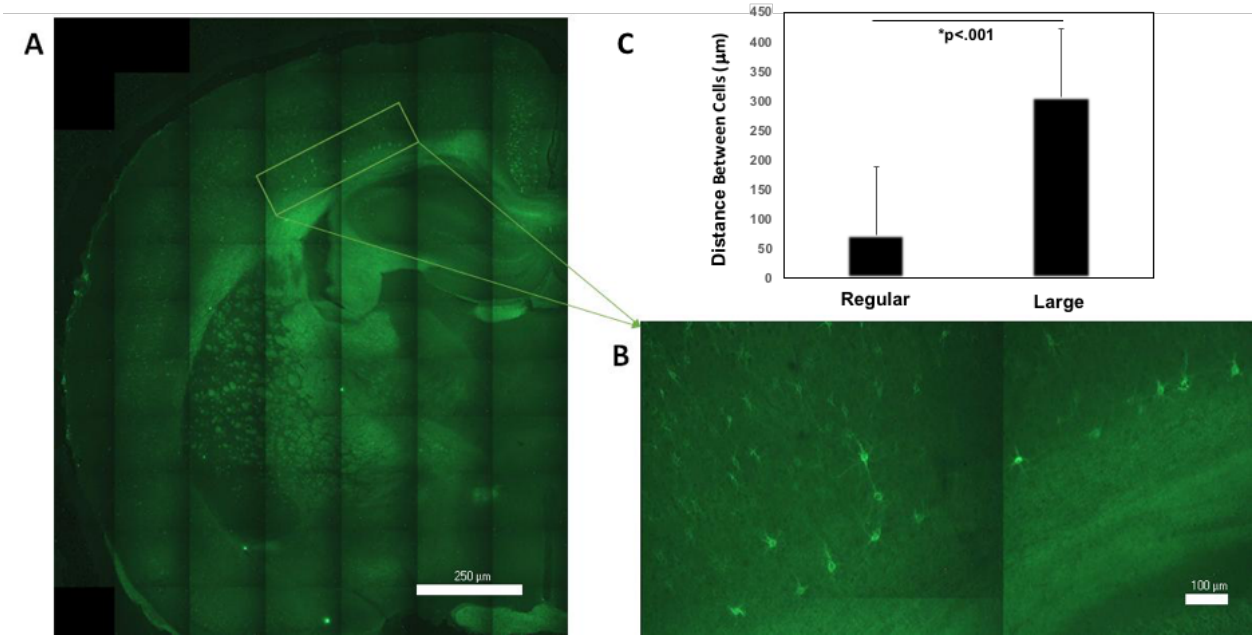

Figure 9. Deep layer staining.

(A) Left hemisphere of adult male Long Evans rat shown, brightly stained PNN ensheathed sub-plate cells are highlighted in box. (B) Larger cells were consistently observed in the deepest part of the neocortex. White arrow pointing to large wfa+ cells and black arrow pointing to a regular wfa+ cell. (C) Distance between regular wfa+ and large wfa+ cells were significantly different ($p<0.001$).

Table 1

ABBREVIATIONS	STRUCTURE NAMES
AID	Agranular insular cx, dorsal
AIP	Agranular insular cx, posterior
AIV	Agranular insular cx, ventral
CG1	Cingulate cortex area 1
CG2	Cingulate cortex area 2
CL	Claustrum
CORTEX LAYERS	Cortex layers
CPU	Caudate putamen (striatum)
DCL	Dorsal part of claustrum
DEN	Dorsal endopiriform nu
DI	Dysgranular insular cortex
EC	External capsule
FMI	Forceps minor of the corpus callosum
FR3	Frontal cortex area 3
GI	Granular insular cortex
IEN	Intermediate endopiriform nu
IL	Infralimbic cortex
LO	Lateral orbital cortex
M1	Primary motor cortex
M2	Secondary motor cortex
PIR 1,2,3	Piriform cortex, layers 1,2,3
PRL	Prelimbic cortex
REGC	Retrospenial granular cortex c
RSD	Retrospenial dysgranular cortex
S1	Primary somatosensory cortex
S1J	Primary somatosensory cortex Jaw region
S1FL	Primary somatosensory cortex Forelimb
S1DZ	Primary somatosensory cortex Dysgranular
S1DZO	Primary somatosensory cortex Oral dysgranular
S1ULP	Primary somatosensory cortex Upper lip
S1TR	Primary somatosensory cortex Trunk regions
S1BF	Primary somatosensory cortex Barrel field
S2	Secondary somatosensory cortex
VCL	Ventral part of claustrum
VO	Ventral orbital cortex

Table 1. Abbreviations of cortical areas that were looked at in this study.

References

Alcaide, J., Guirado, R., Crespo, C., Blasco-Ibanez, J.M., Varea, E., Sanjuan, J., Nacher, J. (2019) Alterations of perineuronal nets in the dorsolateral prefrontal cortex of neuropsychiatric patients. International journal of bipolar disorders, 7,24.

Al-Ghoul, W.M., Miller, M.W. (1989) Transient expression of Alz-50 immunoreactivity in developing rat neocortex: a marker for naturally occurring neuronal death? Brain Research. 481, 361-367.

Alpár, A., Gärtner, U., Härtig, W., Brückner, G. (2006) Distribution of pyramidal cells associated with perineuronal nets in the neocortex of rat. Brain Research 1120(1):13-22.

Andersen, S.L. (2003) Trajectories of brain development: point of vulnerability or window of opportunity? Neurosci Biobehav Rev. 2003 Jan-Mar;27(1-2):3-18.

Anlar, B., Gunel-Ozcan, A. (2012) Tenascin-R: role in the central nervous system. Int J Biochem Cell Biol. 2012 Sep;44(9):1385-9.

Baig, S., Wilcock, G.K., Love, S. (2005) Loss of perineuronal net N-acetylgalactosamine in Alzheimer's disease. Acta Neuropathol. 2005 Oct;110(4):393-401.

Balmer, T.S., Carels,V.M., Frisch, J.L., Nick, T.A. (2009) Modulation of perineuronal nets and parvalbumin with developmental song learning. J Neuroscience 29, 12878-12885.

Bartus, K., James, N.D., Bosch, K.D., Bradbury, E.J. (2011). Chondroitin sulfate proteoglycans: key modulators of spinal cord and brain plasticity. Experimental Neurology.

Bayer, S.A., Altman. J. (1990) Development of layer I and the subplate in the rat neocortex. Exp Neurol. 107, 48-62.

Berretta, S., Pantazopoulos, H., Lange, N. (2007) Neuron numbers and volume of the amygdala in subjects diagnosed with bipolar disorder or schizophrenia. Biol Psychiatry. 2007 Oct 15;62(8):884-93.

Berretta, S., Pantazopoulos, H., Markota, M., Brown, C., Batzianouli, ET. (2015). Losing the sugar coating: potential impact of perineuronal net abnormalities on interneurons in schizophrenia. Schizophrenia Research. 167, 18–27.

Bertolotto, A., Manzardo, E., Guglielmone, R. (1996). Immunohistochemical mapping of perineuronal nets containing chondroitin unsulfated proteoglycan in the rat central nervous system. Cell Tissue Res. 283, 283-295.

Bliss, T.V.P., Cooke, Sam, F. (2011) Long-term potentiation and long-term depression: a clinical perspective. CLINICS. 66, S1, 3-17.

Bradbury, E.J., Carter, L.M. (2011) Manipulating the glial scar: Chondroitinase ABC as a therapy for spinal cord injury. Brain Research Bulletin. Vol 84, Issue 4-5, pp 306-316.

Bradbury, E.J., Moon. L.F., Popat, R.J., King, V.R., Bennett, G.S., Patel, P.N., McMahon, S.B. (2002) Chondroitinase ABC promotes functional recovery after spinal cord injury. Nature. 416; 6881, 636.

Brauer, K., Hartig, W., Bigl, V., Brückner, G. (1993) Distribution of parvalbumin-containing neurons and lectin-binding perineuronal nets in the rat basal forebrain. Brain Res. Dec;631(1) 167-170.

Brauer, K., Hartig, W., Fritschy, J.M., Brückner, G., Bigl, V. (1995) Co-occurrence of perineuronal nets with GABAA receptor alpha 1 subunit-immunoreactive neurons in the rat septal region. Neuroreport. Mar;6(5) 733-736.

Brauer, K., Holzer, M., Brückner, G., Tremere, L., Rasmusson, D.D., Poethke, R., Arendt, T., Hartig, W. (1999) Two distinct populations of cholinergic neurons in the septum of raccoon (Procyon lotor): Evidence for a separate subset in the lateral septum. J. Comp. Neurol., 412: 112-122.

Brecht, M. (2007) Barrel cortex and whisker-mediated behaviors. Current Opinion in Neurobiology. 17, 408-416.

Bruckner, G., Brauer, K., Härtig, W., Wolff, J.R., Rickmann, M.J., Derouiche, A., Delpech, B., Girard, N. Oertel., W.H, Reichenbach, A. (1993) Perineuronal nets provide a polyanionic, glia-associated form of microenvironment around certain neurons in many parts of the rat brain. Glia. 8, 183-200.

Bruckner, G., Bringmann, A., Hartig, W., Koppe, G., Delpech, B., Brauer, K. (1998) Acute and long-lasting changes in extracellular-matrix chondroitin-sulphate proteoglycans induced by injection of chondroitinase ABC in the adult rat brain. Exp Brain Research. 121:3,300-10.

Bruckner, G., J. Grosche, S. Schmidt, W. Hartig, R. U. Margolis, B. Delpech, C. I. Seidenbecher, R. Czaniera, and M. Schachner. (2000) Postnatal development of perineuronal nets in wild-type mice and in a mutant deficient in tenascin-R. J. Comp. Neurol. 428:616–629.

Bruinsma, I.B., Riet, T.L., Gevers, T., Dam, T. G.B., van Kuppevelt, T.H., David, G., Küsters, B., de Waal, R.M., Verbeek, M.M. (2010) Sulfation of heparan sulfate associated with amyloid-beta plaques in patients with Alzheimer's disease. Acta Neuropathol. Feb;119(2):211-20.

Bukalo, O., Schachner, M., Dityatev, A. (2001) Modification of extracellular matrix by enzymatic removal of chondroitin sulfate and by lack of tenascin-R differentially affects several forms of synaptic plasticity in the hippocampus. Neuroscience. 104, 359-369.

Carmichael, S. T., Archibeque, I., Luke, L., Nolan, T., Momiy, J., Li, Songlin. (2005) Growth-associated gene expression after stroke: evidence for a growth-promoting region in peri-infarct cortex,Experimental Neurology,Volume 193, Issue 2,Pages 291-311.

Carulli, D., Kwok, J.C., Pizzorusso, T. (2016) Perineuronal nets and CNS plasticity and repair. Neuronal Plasticity. 4327082.

Carulli, D., Pizzorusso, T., Kwok, J.C.F., Putignano, E., Poli, A., Forostyak, S., Andrews, M.R., Deepa, S.S., Glant, T.T., Fawcett, J.W. (2010) Animals lacking link protein have attenuated perineuronal nets and persistent plasticity. *Brain*, Volume 133, Issue 8, Pages 2331–2347.

Carulli, D., Rhodes, K., Brown, D., Bonnert, T., Pollack, S., Oliver, K., Strata, P., Fawcett, J. (2006) Composition of perineuronal nets in the adult rat cerebellum and the cellular origin of their components. The Journal of Comparative Neurology, 494, 559–577.

Castro-Alamancos, M.A., Donoghue, J.P., Connors, B.W. (1995) Different forms of synaptic plasticity in somatosensory and motor areas of the neocortex. J Neurosci. 15:5324-33.

Celio, M.R., Chiquet-Ehrismann, R. (1993) 'Perineuronal nets' around cortical interneurons expressing parvalbumin are rich in tenascin. Neurosci Lett. 162,137–140.

Celio, M.R., Spreafico, R., Biasi, S.D., Vitellaro-Zuccarello, L. (1998) Perineuronal nets: past and present. Trends Neurosci. 21, 510-515.

Chen, C.C., Abrams, S., Pinhas, A., Brumberg, J.C. (2009) Morphological heterogeneity of layer VI neurons in mouse barrel cortex. J Comp Neurol. 512:726-46.

Chu, P., Farah, S., Ali, S., Wahid, A., Brumberg, J.C. (2015). A Effect of sensory enrichment on perineuronal nets recovery following prolonged sensory deprivation. Program No. 569.28/A99. Neuroscience Meeting Planner. Chicago, IL: Society for Neuroscience.

Chu, P., Abraham, R., Budhu, K., Khan, U., De Marco, Garcia, N., Brumberg, J.C. (2018) The Impact of Perineuronal Net Digestion Using Chondroitinase ABC on the Intrinsic Physiology of Cortical Neurons. Neuroscience. Sep 15; 388:23-35.

Crair, M.C., Malenka, R.C. (1995) A critical period for long-term potentiation at thalamocortical synapses. Nature. 375:325-8.

Dauth, S., Grevesse, T., Pantazopoulos, H., Campbell, P.H., Maoz, B.M., Berretta, S., Parker, K.K. (2016) Extracellular matrix protein expression is brain dependent. Journal of Comparative Neurology. 524:7,1309-1335.

Dityatev, A., Bruckner, G., Dityateva, G., Grosche, J., Kleene, R., Schachner, M. (2007) Activity-dependent formation and functions of chondroitin sulfate-rich extracellular matrix of perineuronal nets. Develop Neurobiol. 67,570-588.

Dityatev, A., Schachner, M. (2003) Extracellular matrix molecules and synaptic plasticity. Nat Rev Neurosci. 4,456–468.

Fader, S. M., Imaizumi, K., Yanagawa, Y., Lee, C, C. (2016). Wisteria Floribunda Agglutinin-Labeled Perineuronal Nets in the Mouse Inferior Colliculus, Thalamic Reticular Nucleus and Auditory Cortex. Brain sciences, *6*(2), 13.

Fatemi, S, H., Earle, J.A., McMenomy, T. (2000) Reduction in Reelin immunoreactivity in hippocampus of subjects with schizophrenia, bipolar disorder and major depression. Mol Psychiatry. Nov;5(6):654-63, 571.

Fatemi, S.H., Stary, J.M., Halt, A.R., Realmuto, G.R. (2001) Dysregulation of Reelin and Bcl-2 proteins in autistic cerebellum. J Autism Dev Disord. Dec;31(6):529-35.

Fawcett, J.W., Oohashi, T., Pizzorusso, T. (2019) The roles of perineuronal nets and the perinodal extracellular matrix in neuronal function. Nat Rev Neurosci 20, 451–465.

Ferrer, I., Bernet, E., Soriano, E., Del Rio, T., Fonseca, M. (1990) Naturally occurring cell death in the cerebral cortex of the rat and removal of dead cells by transitory phagocytes. Neuroscience. 39,451- 458.

Folsom, T. D., Fatemi, S. H. (2013) The involvement of Reelin in neurodevelopmental disorders. Neuropharmacology, 68, 122-135.

Fox, K. (2002) Anatomical pathways and molecular mechanisms for plasticity in the barrel cortex. Neuroscience.111(4):799-814.

Frantz, C., Stewart, K.M., Weaver, V.M. (2010) The extracellular matrix at a glance. Journal of Cell Science 2010 123: 4195-4200.

Frischknecht, R., Heine, M., Perrais, D., Seidenbecher, C.I., Choquet, D., Gundelfinger, E.D. (2009) Brain extracellular matrix affects AMPA receptor lateral mobility and short-term synaptic plasticity. Nat Neurosci. 12,897–904.

Galtrey, C.M., Fawcett, J.W. (2007) The role of chondroitin sulfate proteoglycans in regeneration and plasticity in the central nervous system. Brain Res Rev. 54:1,1–18.

Galtrey, C.M., Kwok, J.C., Carulli, D., Rhodes, K.E., Fawcett, J.W. (2008) Distribution and synthesis of extracellular matrix proteoglycans, hyaluronan, link proteins and tenascin-R in the rat spinal cortex. Eur J Neuroscience 27: 1373-1390.

Gogolla, N., Caroni, P., Lüthi, A., Herry, C. (2009) Perineuronal nets protect fear memories from erasure. Science. 325:5945,1258–1261.

Hartig, W., Appel, S., Suttkus, A., Grosche, J., Michalski, D. (2016) Abolished perineuronal nets and altered parvalbumin-immunoreactivity in the nucleus reticularis thalami of wildtype and 3xTg mice after experimental stroke, Neuroscience, Volume 337, 66-87.

Hartig, W., Brauer, K., Bruckner, G. (1992) Wisteria floribunda agglutinin labelled nets surround parvalbumin-containing neurons. Neuroreport. 3,869 – 872.

Hausen, D., Bruckner, G., Drlicek M., Hartig, W., Brauer K., Bigl, V. (1996) Pyramidal cells ensheathed by perineuronal nets in human motor and somatosensory cortex. NeuroReport 7, 1725-1725.

Hensch, TK. (2003) Controlling the critical period. Neurosci Res. 47,17–22.

Hensch, T. (2005) Critical period plasticity in local cortical circuits. Nat Rev Neurosci 6, 877–888.

Hilbig, H., Bidmon, H.J., Blohm, U., Zilles, K. (2001) Wisteria Wisteria floribunda agglutinin labeling patterns in the human cortex: a tool for revealing areal borders and subdivisions in parallel with immunocytochemistry. Anat Embryol (Berl). 203:1,45-52.

Hjornevik, T., Leergaard, T.B., Darine, D., Moldestad, O., Dale, A.M., Willoch, F., Bjaalie, J.G. (2007) Three-dimensional atlas system for mouse and rat brain imaging data. Front Neuroinform. 2, 1:4.

Hubel, D.H., Wiesel, T.N., LeVay, S. (1977) Plasticity of ocular dominance columns in monkey striate cortex. Philos Trans R Soc Lond B Biol Sci. Apr 26;278(961):377-409.

Hylin, M.J., Orsi, S.A., Moore, A.N., Dash, P.K. (2013) Disruption of the perineuronal net in the hippocampus or medial prefrontal cortex impairs fear conditioning. Learn Mem. Apr 16;20(5):267-73.

Izquierdo, I., Furini, C.R., Myskiw, J. C. (2016) Fear Memory. Physiol Rev. Apr;96(2):695-750.

Jones, C.L., Liu, J., Xu, D. (2010) Comprehensive Natural Products II,6.14 - Structure, Biosynthesis, and Function of Glycosaminoglycans, Elsevier, Pages 407-427, ISBN 9780080453828.

John, N., Krugel, H., Frischknecht, R., Smalla, K. H., Schultz, C., Kreutz, M. R., Gundelfinger, E. D., Seidenbecher, C. I. (2006). Brevican-containing perineuronal nets of extracellular matrix in dissociated hippocampal primary cultures. Molecular and cellular neurosciences, 31(4), 774–784.

Kanold, P.O., Kara, P., Reid, C.R., Shatz. (2003) Role of subplate neurons in functional maturation of visual cortical columns. Science. 301:521-5.

Kanold, P.O. (2004) Transient microcircuits formed by subplate neurons and their role in functional development of thalamocortical connections. Neuroreport. 15, 2149-2153.

Karetko, M., Skangiel-Kramska, J. (2009) Diverse functions of perineuronal nets. Acta Neurobiol Exp. 69, 564-577.

Karetko, M., Skangiel-Kramska, J., Nowicka, D. (2014) Aging somatosensory cortex displays increased density of wfa-binding Perineuronal nets associated with gad-negative neurons. Neuroscience. 277, 734-746.

Katche, C., Dorman, G., Slipczuk, L., Cammarota, M., Medina, J.H. (2017) Functional integrity of the retrosplenial cortex is essential for rapid consolidation and recall of fear memory. Learning & Memory. 20,170 –173.

Kosaka, T., Heizmann, C.W. (1989) Selective staining of a population of parvalbumin-containing GABAergic neurons in the rat cerebral cortex by lectins with specific affinity for terminal N-acetylgalactosamine. Brain Res. Mar 27;483(1):158-63.

Kwok, J.C., Carulli, D., Fawcett, J.W. (2010) In vitro modeling of perineuronal nets: hyaluronan synthase and link protein are necessary for their formation and integrity. J Neurochem. 114(5):1447-1459.

Lander, C., Kind, P., Maleski, M., Hockfield, S. (1997) A family of activity-dependent neuronal cell-surface chondroitin sulfate proteoglycans in cat visual cortex. J Neurosci. 17,1928–1939.

Lau, B. Y. B., Layo, D.E., Emery, B., Everett, M., Kumar, A., Stevenson, P., Reynolds, K.G., Cherosky, A., Bowyer, S.H., Roth, S., McCord, D.G., McCord, R.P., Krishnan, K. (2020). Lateralized Expression of Cortical Perineuronal Nets during Maternal Experience is Dependent on MECP2. eNeuro 24 April 2020, 7 (3) ENEURO.0500-19.

Lensjo, K.K., Christensen, A.C., Tennoe, S., Fyhn, M., Hafting, T. (2017) Differential expression and cell-type specificity of perineuronal nets in hippocampus, medial entorhinal cortex, and visual cortex examined in the rat and mouse. eNeuro. 7, 4(3) 0379-16.

Lipachev, N., Arnst, N., Melnikova, A. et al. (2019) Quantitative changes in perineuronal nets in development and posttraumatic condition. J Mol Hist 50**,** 203–216 (2019).

Lundell, A., Olin, A.I., Morgelin, M., Al-Karadaghi, S., Aspberg, A., Logan, D.T. (2004) Structural basis for interactions between tenascins and lectican C-type lectin domains: evidence for a crosslinking role for tenascins. Structure. 12(8):1495–1506.

Massey, J.M., Hubscher, C.H., Wagoner, M.R., Decker, J.A., Amps, J., Silver, J., Onifer, S.M. (2006) Chondroitinase ABC digestion of the perineuronal net promotes functional

collateral sprouting in the cuneate nucleus after cervical spinal cord injury. J Neurosci. 26, 4406-4414.

Mateos-Aparicio, P., Rodríguez-Moreno, A. (2019) The Impact of Studying Brain Plasticity. Frontiers in Cellular Neuroscience. Vol 13, pp 66.

Matthews, R.T., Kell,y G.M., Zerillo, C.A., Gray, G., Tiemeyer, M., Hockfield, S. (2002) Aggrecan glycoforms contribute to the molecular heterogeneity of perineuronal nets. J Neurosci. Sep 1;22(17):7536-47.

Mauney, S.A., Athanas, K.M., Pantazopoulos, H., Shaskan, N., Passeri, E., Berretta, S., Woo, T.U. (2013) Developmental pattern of perineuronal nets in the human prefrontal cortex and their deficit in schizophrenia. Biol Psychiatry.74, 427–435.

McRae, P.A., Porter, B.E. (2012) The perineuronal net component of the extracellular matrix in plasticity and epilepsy. Neurochem Int. 61(7): 963-972.

McRae, P.A., Rocco, M.M., Kelly, G., Brumberg, J.C., Matthews, R.T. (2007) Sensory deprivation alters aggrecan and perineuronal net expression in the mouse barrel cortex. The Journal of Neuroscience. 27(20):5405-5405.

McQuillen, P.S., Ferriero, D.M. (2005) Perinatal subplate neuron injury: implications of cortical development and plasticity. Brain Pathol. 15, 250-260.

Morawski, M., Bruckner, G., Jager, C., Seeger, G., Matthews, R.T., Arendt, T. (2012) Involvement of perineuronal and perisynaptic extracellular matrix in alzheimer's disease neuropathology. Brain Pathology, 22, 547-561.

Morawski, M., Bruckner, M.K., Riederer, P., Bruckner, G., Arend. (2004) Perineuronal nets potentially protect against oxidative stress. Exp Neurol. 188(2): 309-15.

Morawski, M., Brückner, G., Jäger, C., Seeger, G., Arendt, T. (2010) Neurons associated with aggrecan-based perineuronal nets are protected against tau pathology in subcortical regions in Alzheimer's disease. Neuroscience. Sep 1;169(3):1347-63.

Morawski, M., Dityatev, A., Hartlage-Rübsamen, M., Blosa, M., Holzer, M., Flach, K., Pavlica, S., Dityateva, G., Grosche, J., Brückner, G., & Schachner, M. (2014) Tenascin-R promotes assembly of the extracellular matrix of perineuronal nets via clustering of aggrecan. Philosophical transactions of the Royal Society of London. Series B, Biological sciences, 369(1654), 20140046.

Naffah-Mazzacoratti, M.G., Argañaraz, G.A., Porcionatto, M.A., Scorza, F.A., Amado, D., Silva, R., Bellissimo, M.I., Nader, H.B., Cavalheiro, E.A. (1999) Selective alterations of

glycosaminoglycans synthesis and proteoglycan expression in rat cortex and hippocampus in pilocarpine-induced epilepsy. Brain Res Bull. Nov 1;50(4):229-39.

Nakamura, M., Nakano, K., Morita, S., Nakashima, T., Oohira, A., Miyata, S. (2009) Expression of chondroitin sulfate proteoglycans in barrel field of mouse and rat somatosensory cortex. Brain Res 1252:117–129.

Naskar, S., Narducci, R., Balzani, E. et al. (2019) The development of synaptic transmission is time-locked to early social behaviors in rats. Nat Commun 10, 1195.

Nowicka, D., Soulsby, S., Skangiel-Kramska, J., & Glazewski, S. (2009) Parvalbumin containing neurons, perineuronal nets and experience-dependent plasticity in murine barrel cortex. The European Journal of Neuroscience. 30(11), pp 2053–63.

O'Donnell, W.T., Warren, S.T. (2002) A decade of molecular studies of fragile X syndrome. Annu Rev Neurosci. 25:315-38.

Pantazopoulos, H., Berretta, S. (2016) In Sickness and in Health: Perineuronal Nets and Synaptic Plasticity in Psychiatric Disorders. Neural plasticity, 2016, 9847696.

Pantazopoulos, H., Markota, M., Jaquet, F., Ghosh, D., Wallin, A., Santos, A., Caterson, B., Berretta, S. (2015) Aggrecan and chondroitin-6-sulfate abnormalities in schizophrenia

and bipolar disorder: a postmortem study on the amygdala. Transl Psychiatry. Jan 20;5(1):e496.

Pantazopoulos, H., Woo, T. U., Lim, M. P., Lange, N., Berretta, S. (2010) Extracellular matrix-glial abnormalities in the amygdala and entorhinal cortex of subjects diagnosed with schizophrenia. Archives of general psychiatry, 67(2), 155–166.

Park, H., Kim, M., Kim, H. J., Lee, Y., Seo, Y., Pham, C. D., Lee, J., Byun, S. J., Kwon, M. H. (2017) Heparan sulfate proteoglycans (HSPGs) and chondroitin sulfate proteoglycans (CSPGs) function as endocytic receptors for an internalizing anti-nucleic acid antibody. Scientific reports, *7*(1), 14373.

Pearlman, A.L., Sheppard, A.M. (1996) Extracellular matrix in early cortical development. Prog Brain Res. 108, 117–134.

Peterson, C.C. (2007) The functional organization of the barrel cortex. Neuron. Volume 56, Issue 2, pp 339-355.

Pizzorusso, T., Medini, P., Berardi, N., Chierzi, S., Fawcett, J.W., Maffei, L. (2002) Reactivation of ocular dominance plasticity in the adult visual cortex. Science. 298, 1248–1251.

Pizzorusso, T., Medini, P., Landi, S., Baldini, S., Berardi, N., Maffei, L. (2006) Structural and functional recovery from early monocular deprivation in adult rats. Proc Natl Acad Sci. USA. 103, 8517–8522.

Pothuizen, H.H., Davies, M., Albasser, M.M., Aggleton, J.P., Vann, S.D. (2009) Granular and dysgranular retrosplenial cortices provide qualitatively different contributions to spatial working memory: evidence from immediate-early gene imaging in rats. Eur.J. Neurosci. 30, 877–888.

Rankin-Gee, E.K., McRae, P.A., Baranov, E., Rogers, S., Wandrey, L., Porter, B.E. (2015) Perineuronal net degradation in epilepsy. Epilepsia. Jul;56(7):1124-33.

Romberg, C., Yang, S., Melani, R., Andrews, M.R., Horner, A.E., Spillantini, M.G., Bussey, T.J., Fawcett, J.W., Pizzorusso, T., Saksida, L.M. (2013) Depletion of perineuronal nets enhances recognition memory and long-term depression in the perirhinal cortex. J Neurosci. 33, 7057- 7065.

Rybakowski, J.K., Remlinger-Molenda, A., Czech-Kucharska, A., Wojcicka, M., Michalak, M., Losy, J. (2013) Increased serum matrix metalloproteinase-9 (MMP-9) levels in young patients during bipolar depression. J Affect Disord. Apr 5;146(2):286-9.

Seeger, G., Brauer, K., Härtig, W., Brückner, G. (1994) Mapping of perineuronal nets in the rat brain stained by colloidal iron hydroxide histochemistry and lectin cytochemistry. Neuroscience 58: 371-388.

Semple, B. D., Blomgren, K., Gimlin, K., Ferriero, D. M., Noble-Haeusslein, L. J. (2013). Brain development in rodents and humans: Identifying benchmarks of maturation and vulnerability to injury across species. Progress in neurobiology, 106-107, 1–16.

Slaker, M., Blacktop, J.M., Sorg, B.A. (2016) Caught in the Net: Perineuronal Nets and Addiction. Neural Plast.; 2016:7538208.

Slaker, M.L., Harkness, J.H., Sorg, B.A. (2016) A standardized and automated method of perineuronal net analysis using Wisteria floribunda agglutinin staining intensity, IBRO Reports,Volume 1, Pages 54-60.

Sorg, B. A., Berretta, S., Blacktop, J. M., Fawcett, J. W., Kitagawa, H., Kwok, J. C., Miquel, M. (2016) Casting a wide net: role of perineuronal nets in neural plasticity. Journal of Neuroscience, 36:11459-11468.

Spicer, A.P., Joo, A., Bowling Jr, R.A. (2003) A Hyaluronan Binding Link Protein Gene Family Whose Members Are Physically Linked Adjacent to Chrondroitin Sulfate Proteoglycan Core Protein Genes the missing link. The Journal of Biological Chemistry. 278, 21083-21091.

Tewari, B. P., Sontheimer, H. (2019). Protocol to Quantitatively Assess the Structural Integrity of Perineuronal Nets ex vivo. Bio-protocol 9(10): e3234.

Toyama, B.H., Hetzer, M.W. (2013) Protein homeostasis: live long, won't prosper. Nat Rev Mol Cell Biol. Jan;14(1):55-61.

Tsien, R.Y. (2013) Very long-term memories may be stored in the pattern of holes in the perineuronal nets. Proceedings of the National Academy of Sciences of the United States of America (PNAS). Vol.110 no 30, 12456-12461.

Van den Oever, M.C., Lubbers, B.R., Goriounova, N.A., Li, K.W., Van der Schors, R.C., Loos, M., Riga, D., Wiskerke, J., Binnekade, R., Stegerman, M., Schoffelmeer, A.N.M., Mansvelder, H.D., Smit, A.B., De Vries, T.J., Spijker, S. (2010) Extracellular matrix plasticity and GABAergic inhibition of prefrontal cortex pyramidal cells facilitates relapse to heroin seeking. Neuropsychopharmacology. 35, 2120-2133.

Van Groen, T., Wyss, J.M. (2003) Connections of the retrosplenial granular b cortex in the rat. J. Comp. Neurol. 463, 249–263.

Vann, S.D., Aggleton, J.P., Maguire, E.A. (2009) What does the retrosplenial cortex do? Nat Rev Neurosci. 10, 792 –802.

Vitellaro-Zuccarello, L., De Biasi, S., Spreafico, R. (1998) One hundred years of Golgi's "perineuronal nets": history of a denied structure. Ital J Neurol Sci. 19, 249-253.

Wang, D., Ichiyama, R.M., Zhao, R., Andrews, M.R., Fawcett, J.W. (2011) Chondroitinase combined with rehabilitation promotes recovery of forelimb function in rats with chronic spinal cord injury. J Neurosci. Jun 22;31(25):9332-44.

Wang, D., Fawcett, J. (2012) The perineuronal net and the control of CNS plasticity. Cell Tissue Res 349, 147–160.

Watanabe, H., Cheung, Sc., Itano, N., Kimata, K., Yamada, Y. (1997) Identification of hyaluronan-binding domains of aggrecan. Journal of Biol Chem. Vol. 272, No. 44, pp. 28057–28065.

Wen, T.H., Afroz, S., Reinhard, S.M., Palacios, A.R., Tapia, K., Binder, D.K., Razak, K.A., Ethell, I.M. (2018) Genetic Reduction of Matrix Metalloproteinase-9 Promotes Formation of Perineuronal Nets Around Parvalbumin-Expressing Interneurons and Normalizes Auditory Cortex Responses in Developing Fmr1 Knock-Out Mice. Cereb Cortex. Nov 1;28(11):3951-3964.

Wen,T. H., Binder, D. K., Ethell I.M., Razak K.A. (2018) The Perineuronal 'Safety' Net? Perineuronal Net Abnormalities in Neurological Disorders. Frontiers in Molecular Neuroscience. Vol 11, 270.

Woolsey, T.A., Van der Loos. H., (1970) The structural organisation of layer IV in the somatosensory region (SI) of the mouse cerebral cortex: the description of a cortical field composed of discrete cytoarchitectonic units. Brain Res. 17, 205–242.

Wright, J.W., Kramar, E.A., Meighan, S.E., Harding, J.W. (2002) Extracellular matrix molecules, long-term potentiation, memory consolidation and the brain angiotensin system. Peptides. 23, 221– 246.

Yabluchanskiy, A., Ma, Y., Iyer, R. P., Hall, M. E., & Lindsey, M. L. (2013) Matrix metalloproteinase-9: Many shades of function in cardiovascular disease. Physiology (Bethesda, Md.), 28(6), 391–403.

Yamagata, T., Saito, H., Habuchi, O., Suzuki, S. (1968) Purification and properties of bacterial chondroitinases and chondrosulfatases. J Biol Chem. 243(7):1523–1535.

Yamawaki, N., Radulovic, J., Shephard, G.M.G. (2016) A corticocortical circuit directly links retrosplenial cortex to m2 in the mouse. J Neuroscience. 36(36): 9365-9374.

Ye, Q., Miao, Q. (2013) Experience-dependent development of perineuronal nets and chondrotin sulfate proteoglycan receptors in mouse visual cortex. Matrix Biology. Vol 32, Issue 6, pp 352-363.

Zarrinpar, A., Callaway, E.M. (2006) Local connections to specific types of layer 6 neurons in the rat visual cortex. Journal of Neurophysiology. 95, 3, 1751-1761.

Zhang, Z.W., Deschenes, M. (1997) Intracortical axonal projections of lamina VI cells of the primary somatosensory cortex in the rat: a single-cell labeling study. J Neuroscience. 17, 6365– 6379.

Zhang, Z.W., Deschenes, M. (1998) Projections to layer VI of the posteromedial barrel field in the rat: a reappraisal of the role of corticothalamic pathways. Cereb Cortex. 8, 428 – 436.

Zhou, X. H., Brakebusch, C., Matthies, H., Oohashi, T., Hirsch, E., Moser, M., Krug, M., Seidenbecher, C. I., Boeckers, T. M., Rauch, U., Buettner, R., Gundelfinger, E. D., Fassler, R. (2001). Neurocan is dispensable for brain development. Molecular and cellular biology, 21(17), 5970–5978.

Zimmermann, D.R., Zimmermann, D. (2008) Extracellular matrix of the central nervous system: from neglect to challenge. Histochem Cell Biol. 130; 635–653.